Effect of Dispersant and Binder on Fabrication of BZT-0.5BCT Piezoelectric Wafers by Tape Casting Technique

A Thesis Submitted in Partial Fulfillment of the

Requirements for the Degree of

MASTER OF TECHNOLOGY (RESEARCH)

In

Ceramic Engineering

By

SREERAM ABHINAY
(612CR3008)

Under the guidance of

Prof. R Mazumder
&
Prof. Amarnath Sen

DEPARTMENT OF CERAMIC ENGINEERING
NATIONAL INSTITUTE OF TECHNOLOGY, ROURKELA
&
SENSOR AND ACTUATOR DIVISION, CENTRAL GLASS & CERAMIC RESEARCH INSTITUTE, KOLKATA

Department of Ceramic Engineering
NATIONAL INSTITUTE OF TECHNOLOGY,
ROURKELA
Orissa-769008

CERTIFICATE

This is to certify that the thesis entitled ***"Effect of Dispersant and Binder on Fabrication of BZT-0.5BCT Piezoelectric Wafers by Tape Casting Technique"*** submitted by ***Mr. Sreeram Abhinay*** for the degree of **Master of Technology (Research)** in **Ceramic Engineering** to the National Institute of Technology, Rourkela, is a record of bonafide research work carried out by him under my supervision and guidance. His thesis, in my opinion, is worthy of consideration for the award of degree of Master of Technology (Research) in accordance with the regulations of the institute.

The results embodied in this thesis have not been submitted to any other university or institute for the award of a Degree.

Co – Supervisor
Prof. Amarnath Sen
Head of the Department
Sensors and Actuators Division
CGCRI, Kolkata

Supervisor
Prof. R. Mazumder
Associate Professor
Department of Ceramic Engineering
National Institute of Technology,
Rourkela.

Declaration

I hereby declare that my M.Tech (Research) thesis is entitled as "***Effect of Dispersant and Binder on Fabrication of BZT-0.5BCT Piezoelectric Wafers by Tape Casting Technique*".** This thesis is my own work and has not been submitted in any form for another degree or diploma at any university or other institution of tertiary education. Information derived from the published and unpublished work of others has been acknowledged in the text and a list of references given in this thesis.

Sreeram Abhinay

_____ _____

Date Signature

Contents

Acknowledgement

It is with the most sincere thanks to who helped me to make this thesis possible.

I wish to express my deep, sincere gratitude to advisor ***Prof. Ranabrata Mazumder*** for assigning me the project and for his inspiring guidance, constructive criticism and valuable suggestion throughout this research work. I would also like to thank ***Dr. Amarnath Sen***, Head of the Department, Sensors and Actuators Division, CGCRI- Kolkata, for the continuous suggestion to achieve the research objective. I received excellent academic training from them. Thank you sir for your valuable advice and inspiration.

I am also thankful to ***Dr. Anshuman Seal*** Scientist, CGCRI - Kolkata, for his valuable suggestions and encouragements at various stages of the work.

I express my sincere thanks to Prof. Swadesh Pratihar, Head of the Department, Ceramic Engineering for providing me all the departmental facilities required for the completion of the project work. I am also thankful to all other faculty members of the Department of Ceramic Engineering, NIT Rourkela for their constructive suggestions and encouragement at various stages of the work.

My sincere thanks to all non-teaching staffs in Department of Ceramic Engineering for providing full of high- spirited delight in the lab and helping me throughout this project.

My sincere indebted to my senior research colleagues *Ganesh Bhai, G. Jayarao, Abhishek Choudhary, Prativa Adhikari, M. Raju* for their unconditional support and constant motivation whenever needed. I am very grateful to my friends Ch. *Sowjanya, P. Venkatesh, P. Sreenivasulu, T. Sarath Chandra and Satyananda Behera* who have given me their friendship, put up with my odd hours, and provided me with lifts and practical help.

Last but not least, I would like thank to my ***dear parents & my loving sister*** who have patiently extended all kinds of help for accomplishing this work.

S. Abhinay

Abstract

Recently, piezoelectric wafers/substrates have opened new opportunities for nondestructive evaluation (NDE) of structures in defence, aerospace and industrial sectors. Such wafers can be easily made by tape casting of slurries where dispersants and binders play a critical role. Generally, lead zirconate titanate (PZT) based compositions are used for piezo wafers/substrates. However, recent concern about environmental pollution from lead-based materials has generated renewed interest in developing lead-free ferroelectrics like $Ba(Zr_{0.2}Ti_{0.8})O_3$-$0.5(Ba_{0.7}Ca_{0.3})TiO_3$ [BZT-0.5BCT] having high dielectric constant (ε_r>3500) and piezoelectric properties (d_{33}> 500pC/N). To date, there are no reports on the fabrication of BZT-0.5BCT wafers by tape casting and their electrical characterization.

The objective of the thesis is to develop a dense warpage free BZT-0.5BCT wafer/substrate with suitable dielectric and piezoelectric property. The BZT-0.5BCT powder was synthesized by solid-state reaction route. BZT-0.5BCT tapes were fabricated by a non-aqueous tape casting method. Tape casting slurries of BZT-0.5BCT powder were prepared using methyl ethyl ketone-ethanol (MEK-EtOH) (solvent), phosphate ester / polyvinyl butyral (PVB) (dispersant), PVB (binder), polyethylene glycol (PEG) and butyl benzyl phathalate (BBP) (plasticizer). The optimum amount of dispersant was determined from the minimum in slurry viscosity and sedimentation height. The role of the two dispersants (phosphate ester and PVB) in making stable slurry of BZT-0.5BCT powder vis-a-vis the final properties of the fired wafers was studied. It was confirmed that 1 wt.% phosphate ester is sufficient for effective dispersion of BZT-0.5BCT to get stable slurry and the amount was 0.5 wt.% when PVB was used as dispersant in place of phosphate ester. The role of the binder (PVB) on the fabrication of wafer was also studied. Variation of PVB content shows that at least 3wt% PVB required to get the workable green tape. Up to 3.5 wt% PVB (binder) addition, solid loading can be maintained at 65%. Improved dielectric (ε_r =1750 at 1 kHz), ferroelectric (P_r = 6.3 $\mu C/cm^2$), and piezoelectric property (d_{33} =174 pC/N) were observed for wafers made without phosphate ester.

Keywords: BZT-0.5BCT; Tape-Casting; Rheology; Dielectric Properties; Piezoelectric properties;

List of figures

List of Tables

Chapter – 1

Introduction

1.0 Piezoelectricity

The foundation of the word ‘piezo’ signifies "pressure" in Greek; thus the first importance of the word piezoelectricity suggested 'pressure electricity.' Certain materials produce electric charge on their surfaces as a result of applying mechanical stress. The induced charges are proportional to the mechanical stress. This is called the direct piezoelectric effect and was discovered in quartz by Pierre and Jacques Curie in 1880 [1]. They observed this phenomenon in the following crystals: zinc blende, sodium chlorate, boracites, tourmaline, quartz, calamine, topaz, tartaric acid, cane sugar, and Rochelle salt. Additionally these materials exhibit the reverse piezoelectric effect, discovered by Gabriel Lippmann in 1881, i.e., the internal generation of mechanical strain because of applying electrical field [1, 2].

1.0.1 Direct and converse piezoelectric effect

The direct piezoelectric effect happens when a piezoelectric material turns out to be electrically charged when subjected to mechanical stress. This material can be utilized to identify the strain, development, constrain, weight or vibration by building up a fitting electrical response as in the case of acoustic or ultrasonic sensors. The Converse Piezoelectric effect happens when the piezoelectric material gets to be strained when set in an electric field. This property can be utilized to produce strain, development, constrain, weight or vibration through the application of a suitable electric field [1-5].

1.1 Classification based on symmetry

To understand the concept of piezoelectricity in solids starts with knowledge of the crystal structure of the material. For this purpose consider a single crystallite.

In all, there are 230 space groups and just 32-point groups. All the crystals can be divided into these 32-point groups. Out of these 32-poin tgroups, 11 are centrosymmetric, meaning the center of positive and negative charge coincides with each other, whereas the rest 21 are non-centrosymmetric with one or more crystallographically unique directional axes. Out of the 21 non-centrosymmetric point groups, 20 belongs to the class of piezoelectric. Out of these 20-point groups, 10-point groups have a unique crystallographic axis and, therefore, can have an electric dipole even at zero applied field (electrical and mechanical). These are called as pyroelectric. Also in these types of crystals change in temperature causes a change in the spontaneous polarization [9]. Pyroelectric materials include a subclass of materials in which an external

applied field can change the direction of polarization. These materials are referred to as ferroelectric. In ceramic form, only ferroelectric materials show piezoelectricity.

Flow chart showing the classification of point groups on the basis of symmetry[9]

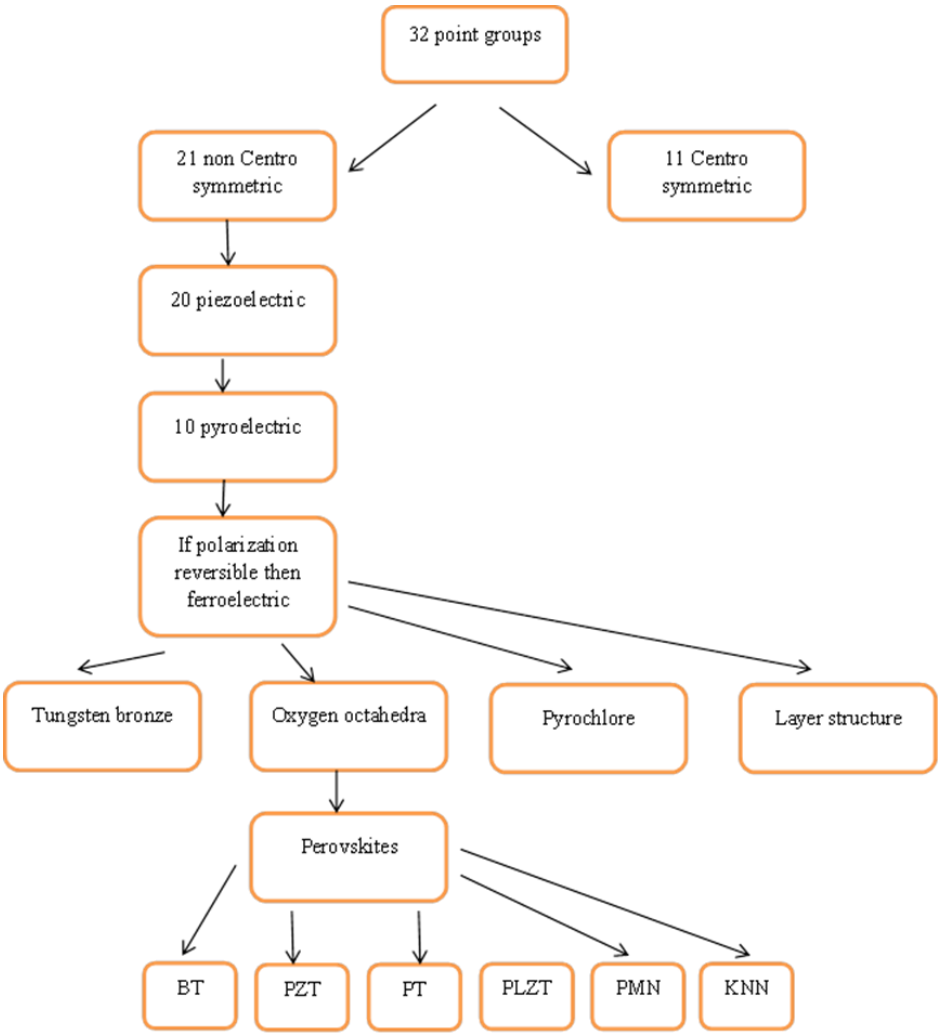

Figure 1.1 Flow chart showing the classification of point groups on the basis of symmetry [5]

Polycrystalline ferroelectric materials in which the crystal axes of the grains are randomly oriented they behave as isotropic materials. If the crystals belong to a piezoelectric class and their crystal axes can be suitably aligned, and then a piezoelectric polycrystalline ceramic becomes possible [5]. A polar direction can be developed in a ferroelectric ceramic by applying a static field; this process is known as ‘poling’. The ‘poling’ process can orient the crystal axis so that the spontaneous polarization has a component in the direction of the poling field [5].

1.2 Piezoelectric coefficients

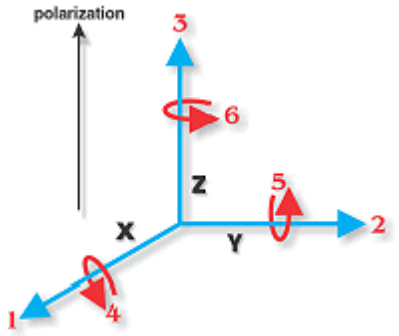

Figure 1.2 Directions of forces affecting a piezoelectric element [5]

Figure 1.2 shows the direction of positive polarization coinciding with the Z-axis of a rectangular system of X, Y and Z axes. Direction X, Y, or Z is represented by numbers 1, 2, and 3 respectively and shear about one of these axes is represented by 4, 5, and 6 respectively [4].

1.2.1Piezoelectric charge constant (d)

The polarization or strain induced in a piezoelectric material by a applied stress or an applied electric field is proportional to the input field (i.e. applied stress or applied electric field), where d is the proportionality constant. The piezoelectric charge constant (d) is the polarization generated per unit of mechanical stress (σ) applied to a piezoelectric material or the mechanical strain (*x*) experienced by a piezoelectric material per unit of electric field applied. The first subscript to d indicates the direction of polarization generated in the material when the electric field E is zero or the direction of applied field strength. The second subscript of d denotes the direction of the applied stress or the induced strain respectively. The piezoelectric constant is an important indicator of materials for strain-dependent (actuator) applications.

For direct piezoelectric effect,

$$P_i = d_{ijk}\sigma_{jk} \qquad (1.3)$$

Where P is the polarization, d_{ijk} is a 3rd rank tensor called as piezoelectric charge coefficient, σ is an applied stress (2nd rank tensor) and the subscripts i, j, k run from 1 to 3 using the Einstein convention.

For converse piezoelectric, d_{33} is written by

Where *x* is the strain $x_{ij} = d_{ijk}E_{jk}$ (1.4)

Developed and E is an applied electric field. The piezoelectric coefficient, d, is numerically identical for both direct and converse piezoelectric effects for free boundary conditions [4].

It should be noted that the notation for the 3rd rank tensor d_{ijk} is often shortened to d_{ij}, where j' = 1, 2, 3, 4, 5, 6 corresponds to jk = 11, 22, 33, 23 or 32, 13 or 31, 12 or 21, respectively (Example $d_{333} = d_{33}$, $d_{311} = d_{31}$) [5].

1.2.2 Piezoelectric Voltage Constant (g)

The piezoelectric voltage constant (g) is the electric field generated by a piezoelectric material in response to an applied physical stress. It is important for assessing a material's suitability for sensing (sensor) applications. The g constant is related to the d constant by the permittivity.

The constant d_{ij} and g_{ij} are related through the equation

$$g_{ij} = \frac{d_{ij}}{\varepsilon_0 \varepsilon_{ij}} \qquad (1.5)$$

Where ε_0 is the permittivity of the free space.

Where g [mV/N] is the piezoelectric voltage constant, d is the piezoelectric charge constant, ε_r is the relative permittivity and ε_0 is the permittivity of free space (8.85×10-12 F/m).

The origin of the piezoelectric effect in ceramics is controlled by the intrinsic and extrinsic effect. Intrinsic effect arises due to the strain produced in the crystal lattice. These intrinsic contributions are reversible and occur without loss [6]. In ferroelectric materials, extrinsic effects are produced due to the motion of domain walls separating regions with different local polarization directions and phase boundary shifts [7]. This effect depends on the frequency, time and applied field and irreversible in nature.

Piezoelectric coefficients such as piezoelectric charge constant, voltage constant, and relative permittivity are temperature dependent.

1.2.3 Electromechanical coupling factor

The Electromechanical coupling factor K_p is an indicator of the effectiveness with which a piezoelectric material converts when an electric field is applied into mechanical energy, or vice versa when mechanical energy is applied [7].

$$K^2 = \frac{Stored\ mechanical\ energy}{Input\ electrical\ energy} \qquad (1.6)$$

Or

$$K^2 = \frac{\boldsymbol{Stored\ electrical\ energy}}{\boldsymbol{Input\ mechanical\ energy}} \qquad (1.7)$$

1.3 Curie temperature

At a specific temperature, about every ferroelectric material go through a ferroelectric paraelectric phase transition.The temperature at which a ferroelectric material returns to the high-temperature paraelectric stage is known as the Curie temperature (T_c) [7, 8, 9]. On cooling through T_c into a ferroelectric stage, a reorientable unconstrained polarization is created. In ferroelectrics dominated by a displacive phase transition, for example, perovskite materials, the temperature dependence of the permittivity changes for 1st and 2nd order phase transitions. Fig. 1.3 outlines the temperature dependence of the permittivity for displacive ferroelectric materials displaying first or second order phase transitions. Second-order phase transitions, which are basic for rhombohedral compositions, are for the most part portrayed by an expansive crest in permittivity. Ferroelectrics is experiencing first order phase transitions, basically for tetragonal perovskite materials, however, show a fairly flat permittivity with increasing temperature right up to the T_c [8, 9].

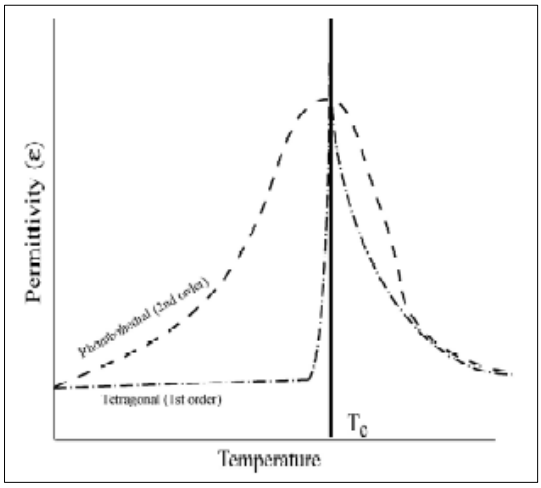

Figure 1.3 Idealized permittivity of a ferroelectric material as a function of temperature [5]

1.4 Ferroelectric hysteresis

Hysteresis loop (PE loop), is a simple and effective tool and the most generally accepted method to understand ferroelectric materials [9, 10]. A polarization-electric field loop is a hysteretic curve showing the variation of electric polarization (C/m^2) with the electric field (V/m). Through the hysteresis loops, the ferroelectricity could be identified directly. Fig.1.4 is a typical ferroelectric hysteresis loop, through which the characteristic parameters, such as spontaneous polarization (P_s), remanent polarization (P_r) and coercive field (E_c) can be determined. The directions of the domains are randomly distributed in such a way to lead to zero net polarization. In the event that an unspoiled sample is subjected to an increasing electric field, the dipoles get to be aligned to the field. When the field has received a certain point, no further increment in polarization is observed because all the dipoles are adjusted towards applied electric field. The material is then said to have come to its saturation limit (P_s). If the field is now reduced to zero, the polarization does not fall to zero but to a value lower than P_s known as remanent polarization (P_r). If the field is now increased in the opposite direction, the polarization of the sample increments in the negative course until it achieves a saturation polarization (–Ps). In the event that the field is again diminished to zero, the polarization tumbles to the remanent polarization For the ideal ferroelectric system, the observed hysteresis loops should be symmetric. The positive and negative E_c and P_r are equal. In reality the shape of ferroelectric hysteresis loops may be effected by many factors such as thickness of the specimen, material composition, thermal treatment, presence of charged defects, mechanical stresses, measurement conditions and so on [8, 9, 10].

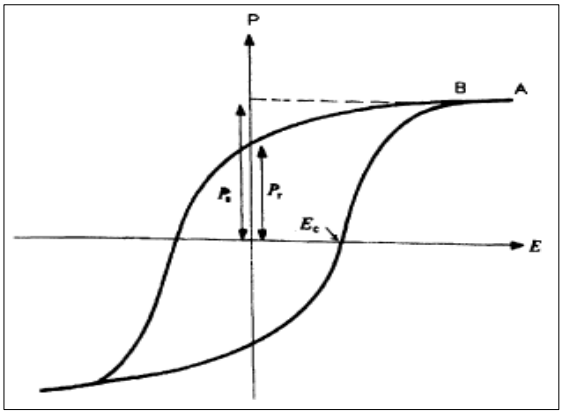

Figure 1.4 Hysteresis loop illustrating the coercive field Ec, the spontaneous polarization Ps, and the remanent polarization Pr. [5]

1.5 Piezoelectric materials

Some typical piezoelectric materials include quartz, Berlinite, Gallium orthophosphate, Tourmaline, Barium Titanate, Lead Zirconate Titanate, Zinc oxide, Aluminium Nitride, Polyvinyl fluoride and Polyvinylidene Fluoride. The piezoelectric ceramics are brittle, and they have better electromechanical properties when compared to the other piezoelectric materials. This segment gives a brief description about the different piezoelectric materials.

1.5.1 Single crystals

Quartz, lithium nibonate ($LiNbO_3$), and lithium tantalate ($LiTaO_3$) are some of the most popular single crystals materials. The single crystals are anisotropic in nature and have distinctive properties relying upon the cut of the materials and course of bulk or surface wave propagation. These materials are essentially used for a frequency stabilized oscillators and surface acoustic device applications [1, 3].

1.5.2 Lead-based Perovskites

Lead-based perovskites form an important class of piezoelectrics. $Pb(Zr_xTi_{1-x})O_3$ (PZT) system and its modified solid solutions are known to exhibit excellent dielectric, elastic and piezoelectric properties at the 'Morphotropic Phase Boundary' (MPB) (fig 1.5)because they have high electromechanical coupling coefficient and high T_c [9, 10]. PZT-based piezoelectric ceramics is popular due to relatively easy to sinter at lower temperatures than other lead-free piezoelectrics and form solid-solution with many different constituents, thus allowing a wide range of achievable properties. But the major drawback of PZT-based ceramics is its high lead content (60 wt%), and PZT is now facing a global restriction because of its lead toxicity. Thus, there is worldwide focus on the development of lead-free materials with electromechanical properties comparable with PZT [11]

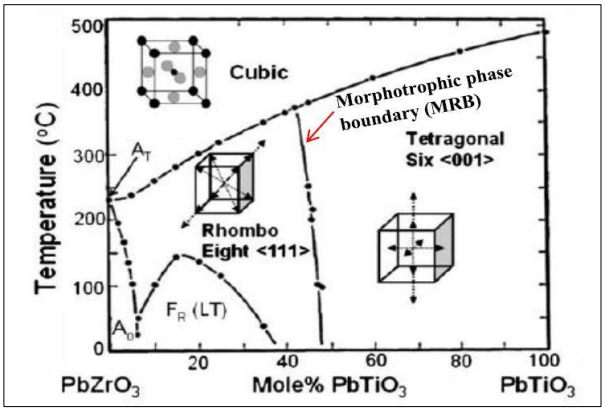

Figure 1.5 Phase diagram of PbZrO3 -PbTiO3 ceramic [5]

1.5.3 Lead-free Piezoelectrics

1.5.3.1 Barium titanate

Since the discovery of ferroelectricity in Barium titanate in 1945, it has been one of the most exhaustively used lead-free material in the electronic industry. It is isostructural with the mineral perovskite $CaTiO_3$ and so is referred as perovskite. A typical ABO_3 structure is given below in fig-1.6 for example $BaTiO_3$ with A at the corners, B at the center and oxygen at the face centers.

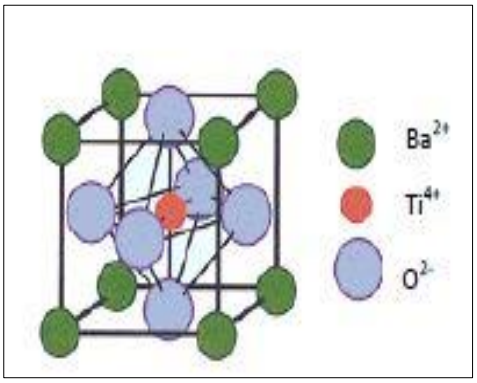

Figure 1.6 Structure of $BaTiO_3$ [5]

Above 120^{o}C this is in cubic structure. However, as the temperature is lowered it undergoes phase transformations to three different ferroelectric phases, each involving small distortions from the cubic symmetry. At 120^{o}C, it undergoes a paraelectric to ferroelectric transition to a tetragonal structure, it is orthorhombic between 5^{o}C and -90^{o}C and finally, it is rhombohedral below -90^{o}C (fig 1.7). Each of these distortions can be thought of as elongations of the cubic unit cell along an edge **(**tetragonal), along a face diagonal (orthorhombic), or along a body diagonal (rhombohedral). These distortions result in a net displacement of the cations with respect to the oxygen octahedra along these directions. It is primarily these displacements that give rise to the spontaneous polarization in the ferroelectric phases [1, 7].

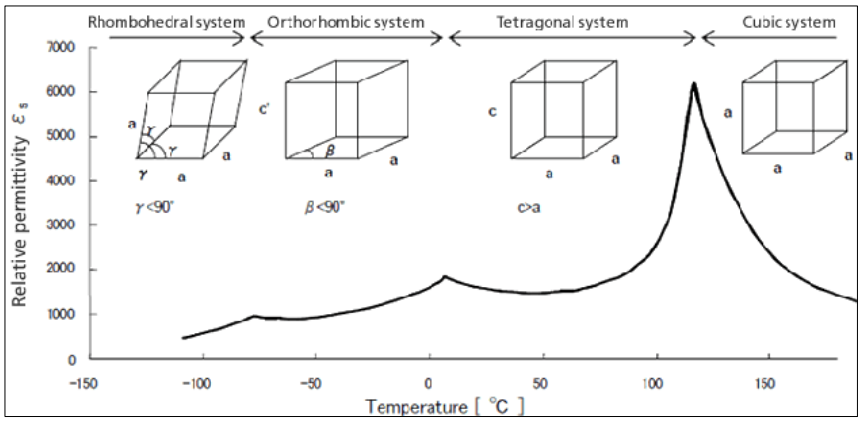

Figure 1.7 Variation of Relative permitivity with temperature [5]

Though $BaTiO_3$ is the first piezoelectric transducer ceramic ever developed, it is not used in piezoelectric devices due to following reason (1) its relatively low T_c of 130°C, which limits its use as high-power transducers, and (2) its low electromechanical coupling factor in comparison to $Pb(Zr_xTi_{1-x})O_3$ (x= 0.52 -0.48), which limits its operational output.

1.5.3.2 Sodium Potassium Niobate (NKN) based materials

Sodium potassium niobate [(Na, K)NbO_3] is the solid solution of ferroelectric potassium niobate ($KNbO_3$ or KN) and antiferroelectric sodium niobate ($NaNbO_3$ or KN) [12]. Both have different orthorhombic structure at room temperature. KNN exhibits an MPB at around 50/50 composition separating two different orthorhombic phases and as for PZT, an increase in the properties for composition near this MPB is observed. NKN shows low piezoelectric properties (d_{33} ~ 80pC/N) due to difficulty in producing dense ceramics. Dense NKN ceramics is difficult to produce because of following two reasons:

1. According to the phase diagram of $KNbO_3$-$NaNbO_3$, phase stability of NKN, is limited to 1140^{o}C.So a high sintering temperature is not possible.
2. NKN system contains volatile elements like Na and K, which result in poor densification.

Apart from above two reasons NKN systems are hygroscopic in nature that further degrade the properties and hinders its applications.

To improve the sinterability and properties of KNN ceramics, various solid solutions such as KNN–$BaTiO_3$, KNN–$LiNbO_3$, KNN–$SrTiO_3$, KNN–$LiTaO_3$, and KNN– $Li(Nb,Ta,Sb)O_3$, KNN–$LiSbO_3$, NKN-$CaTiO_3$, NKN-$BiFeO_3$,NKN-$(Na_{.5}Bi_{.5}TiO_3)$ etc. based composition at the

MPB were used [13]. Saito et al. [14] investigated MPB system between $(K_{0.5}Na_{0.5})NbO_3$, $LiTaO_3$ and $LiSbO_3$, and invented $(K_{0.44}Na_{0.52}Li_{0.04})(Nb_{0.84}Ta_{0.10}Sb_{0.06})O_3$ ceramics with an electric field-induced strain comparable with that of a typical actuator-grade PZT. The ceramic exhibited d_{33} of 300 pC/N, and the texturing of the material led to a peak $d_{33}$of 416 pC/N, and Curie temperature was nearly 253°C.

1.5.3.3 Bismuth Sodium Titanate (BNT) based materials

Bismuth sodium titanate, $(Bi_{0.5}Na_{0.5})TiO_3$ (BNT) is another important lead-free material which has a perovskite structure with strong ferroelectric properties (large remnant polarization (P_r~38 C/cm^2) and high Curie temperature (T_c ~ 320^{o}C). However, BNT-based ceramics undergoes another phase transition below T_c that is known as depolarization temperature (T_d), which often occurs below 200°C.The piezoelectric properties of BNT ceramics are reduced below T_d due to depolarization. This depolarization in BNT ceramics is an important aspect from the application point of view. Fabrication of dense BNT ceramics is difficult as it requires higher sintering temperature above 1200^{o}C which results in loss of Bi from BNT based materials. High leakage currents and high coercive field (E_c=73kV/cm) negatively impact the poling process, and polarization saturation is difficult to achieve in conventionally fabricated $(Bi_{0.5}Na_{0.5})TiO_3$ samples.

Moreover, to improve the piezoelectric properties of BNT, the formation of solid solutions with another perovskite [$BaTiO_3$, $(Bi_{1/2}K_{1/2})TiO_3$, $NaNbO_3$, $BiFeO_3$,etc.] to form an MPB was also studied. Different are expected for the BNT-based. [15, 16].

1.6 Applications of Piezoelectric ceramics

The applications for piezoelectric ceramics are manifold and pervasive, covering all areas of our workplaces, homes, and automobiles. Their applications can be divided into four different groups based on their physical effect used, i.e., generators, motors, combination devices and resonant devices. Generators use of direct piezoelectric effect whereas actuators/motors works on converse piezoelectric effect. Finally, a combination device works on both effects. An overview of all the applications is given in below Table-1.1 [9].

Table 1.1 Applications of Piezoelectric materials

Generators (millivolts to kilovolts)	**Motors (microns to millimeters)**
Hydrophones	Actuators (micro and macro)
Microphones	Loud speakers, tweeters
Phonograph cartridges	Camera shutters, autofocusing
Gas ignitors	Buzzers
Accelerometers	Ink jet printers
Power supplies	Fish finders
Photo flash actuators	Micro positioners
Sensors-environmental, tactile, etc.	Valve controllers
Motor/Generator (combination devices)	Pumps
Sonar	**Resonant devices (kilohertz to megahertz)**
Ranging tranducers	Ultrasonic cleaners
Non-destructive testing (NDT)	Ultrasonic welders
Medical ultrasound	Filters [IF (Intermediate frequency), SAWs (Surface Acoustic Wave)]
Fish finders	Transformer

1.6.1 Piezoelectric materials for structural health monitoring applications

There is a requirement for monitoring of structural health and identification damage for a variety of utilizations running from composite flying vehicles to common and mechanical building frameworks. Structural health monitoring (SHM) or integrated vehicle health monitoring (IVHM) requires small, light-weight, minimally invasive sensors that can be embedded in or mounted on the surface of the structure Fig.-1.8. When an elastic wave travels through a region where there is a change in material properties, scattering occurs in all directions. Active sensing methods utilize the distributed actuator/sensors, permanently attached to the structure, to

generate the elastic wave and measure the arriving waves at sensors. Bulk piezoelectric materials are used for ultrasound based SHM and NDE applications, but the limitation of using bulk materials are difficulty in integrating with the sensor system, the heavy weight of the system and low compliance. However, for the NDE of thin-wall structure, piezoelectric wafers look very promising for Lamb wave excitation and sensing. Piezoelectric wafer active sensors (PWAS) can act as both sensors and actuators [17, 18].

So it will be interesting to study the fabrication of lead-free piezoelectric wafer/substrate by some suitable method and their characterization.

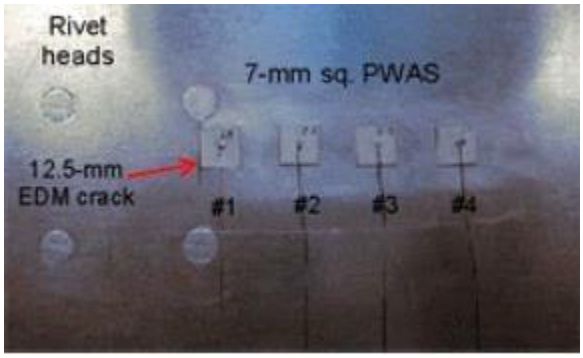

Figure 1.8 Piezoelectric wafer active sensors (PWAS) mounted on an aircraft panel. [18]

1.7 Tape Casting:

Conventional ceramic processing techniques such as dry pressing, extrusion and slip casting are not suitable for preparing thick films with precise dimensional control and a smooth finish. Tape casting is a low-cost method for producing flexible and high quality thin ceramic sheets for which an adequate thickness control and excellent surface finish are required. Tape casting is also known as a doctor blade method because the doctor is a scraping blade for the removal of an excess substance from a moving surface being coated [19,20]. Tape casting involves the preparation of stable slurry in an aqueous or non-aqueous solvent. Usually, the addition of dispersants is required to stabilize the suspension. Tape casting was usually based on a non-aqueous solvent as the dispersing medium. In recent years, there have been some excellent successes with aqueous based tape casting, but in most cases, non-aqueous based systems are used because of higher drying rates [20]. The doctor blade gap between the blade and the carrier defines the wet thickness of the tape being cast. Other variables that come into play include reservoir depth, the speed of carrier movement, and viscosity of the slip and the shape of the doctor blade. On the other hand, to impart adequate strength and flexibility to green tape the addition of binders and plasticizers is important. The most important factors determining the properties of the tape are:

1. Properties of ceramic powder and
2. The compositions of tape casting slurry [1].

The preparation of slurry is carried out in two stages; first the powder is dispersed in the solvent with the help of dispersant and in the second stage binders and plasticizers are added. A homogeneous product can only be obtained if the suspension has high homogeneity and stability and this homogeneity should be preserved in all processing steps such as casting, drying, burn out and sintering. In the present thesis, we restricted our discussion to non-aqueous tape casting only.

1.7.1 Solvent:

The main role of the solvent is to dissolve all the additives added to it, and it should allow the powder to get deagglomerated and to disperse. High dielectric constant (ε) of the solvent is important, as it promotes polarization at the solid-liquid interface that helps in the stabilization of the slurry. In place of single solvent, multiple solvents are used in the preparation of tape casting

slurry to dissolve a wide variety of ingredients. Blends of organic solvents in a particular concentration called azeotropic mixture has dissolving capabilities of all of the solvents, however, evaporates as a single liquid. In addition, mixing of solvents helps in adjusting the dielectric constant, surface tension, and boiling point of final solvent which improves stability, drying rate and lowers cost [20, 22]. Table 1.2 and Table 1.3 summarize the various physical properties of different solvents and boiling points of the different azeotropic mixture with composition, respectively.

Table 1.2: Some physical properties of solvents used

Solvent	**Surface Tension (erg/cm)**	**Dielectric constant**	**Viscosity (mPa.s)**	**Boiling point(^{0}C)**	**Density (gm/cc)**
Water	72.75	78.5	1.0	100	1
Ethyl alcohol		24	1.2	78.4	0.789
Methyl alcohol	22.5	32.6	0.6	64.6	0.789
Methyl ethyl ketone		18	0.4	80	0.805
Acetone	25.1	20.7	2.3	56	0.781
Toluene	28.5	2.4	0.6	110.6	0.867
Isopropyl alcohol	21.4	18.8	2.4	82.3	0.785

Table 1.3: Binary Azeotropic mixtures

Azeotropic mixtures	**Composition**	**Boiling point (^{0}C)**
Methyl ethyl ketone- ethanol	60:40	74.8
Ethanol- Methyl ethyl ketone	60:40	77.3
Isopropyl alcohol- Methyl ethyl ketone	30:70	77.3
Toluene-ethyl alcohol	32:68	76.7
Toluene-ethyl alcohol	73:27	70.9

1.7.2 Dispersant:

The purpose of the dispersant is to disperse primary particles and to hold them in a homogeneous suspension. There are two primary mechanisms involved for the preparation of stable suspension namely; electrostatic stabilization and polymeric stabilization [21-23]. A well-dispersed suspension typically displays a lower viscosity due to the particle mobility offered by the fluid interparticulate layer. Flocs or agglomerates in the slip cause inhomogeneity in the green tape by introducing high porosity regions within the interstitial void space of particle group. The defloculant acts against particle grouping thus increasing homogeneity in the slip, tape, and final part. The optimum amount of dispersant can be found out by rheological study [22]. Measurement of slurry viscosity combined with the sediment height test can be used to judge the relative effectiveness of the dispersant concentration required [19].

1.7.2.1 Electrostatic stabilization

Electrostatic stabilization associated with dissociation of ionizable species in liquid dispersion media and preferential adsorption of ions on the particle surface. To maintain electro neutrality, an equal number of Counter-ions with the opposite charge will surround the colloidal particles and give rise to overall charge-neutral double layers. In charge stabilization, it is the mutual repulsion of these double layers surrounding particles that provides stability.

In particular, Derjaguin, Landau, Verwey, and Overbeek (DLVO) theory explains the generation of net forces by balancing the attractive contribution that arises because of van der Waals forces and repulsive force that is due to overlapping of electrical double layers.

$$V_T = V_A + V_R$$

where V_T is the total potential energy of particle-particle interaction, V_A is van der Waals force of attraction and V_R is the repulsion between the particles.

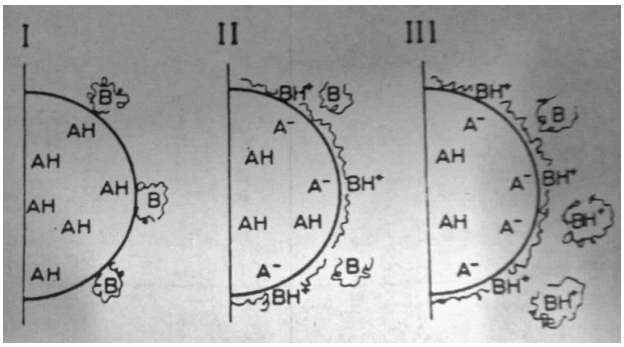

Figure 1.9: Electrostatic charge mechanism [21]

In nonaqueous media, stabilization occurs in the different way, as shown in Fig. 1.9. Here, stabilization takes place in three steps: (1) adsorption of dispersants (usually long-chain acids) on the basic particle surface sites; (2) dissociation of the adsorbed dispersant by transferring protons to the surface sites and (3) in later stage some dissociated anions desorb into the solution leaving a positive charge on the particle surface.

1.7.2.2 Polymeric Stabilization

Polymeric stabilization is a general mechanism that happens in nonaqueous media. Two different ways can achieve polymeric stabilization

1. Steric hindrance – in which the polymer molecule attach to the particle surface.
2. Depletion mechanism – in which polymer molecules are free in suspensions.

In organic solvents, steric stabilization is the effective tool. Adsorbed polymer on the particle surface can accomplish this action by two ways

1. Strong anchoring to the particle surface.
2. Sufficient extension of adsorbed long chain into solution.

However, the success of steric stabilization depends on the surface coverage of the particle, the configuration of the adsorbed polymer and the thickness of adsorbed layer. Menhaden fish oil that contains polyunsaturated ester molecules (glyceryl esters of fatty acids) stabilizes inorganic powders by steric stabilization.

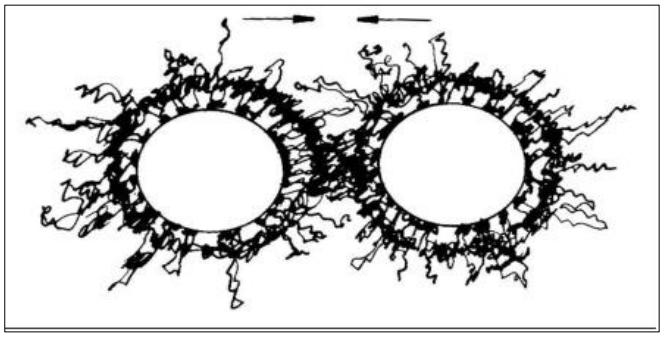

Figure 1.10: steric mechanism [21]

1.7.2.3 Combined stabilization mechanism

The combination of both electrostatic and steric mechanisms can result in better stabilization in which electrostatic component may originate from a net charge on the particle surface and steric component associated with the anchored polymer. In the present work phosphate ester was selected as dispersant that stabilizes in the combined stabilization mechanism [25].

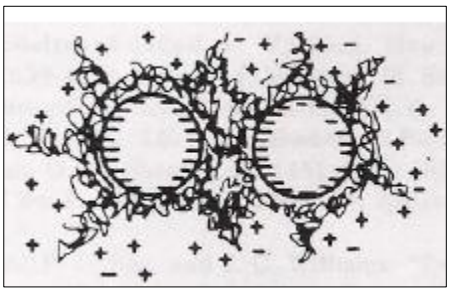

Figure 1.11: Combined stabilization mechanism [21]

1.7.2.4 Phosphate ester:

A phosphate ester is a very powerful dispersant for many oxide powders including $BaTiO_3$, Al_2O_3, and TiO_2 in nonaqueous medium. It is soluble in either water or numerous organic solvents. It disperses powder particles both by ionic and steric hindrance mechanisms. Fig-1.12 shows the typical structure of phosphate ester. Many authors showed that in MEK - Ethanol system, phosphate ester works well and allows relatively high solid loading. The possible mechanism for combined stabilization might be that polymer structure will get physically adsorbed onto the particle surface and then ionizes. One major drawback with phosphate ester is the contamination of ceramic body by residual phosphorous [20].

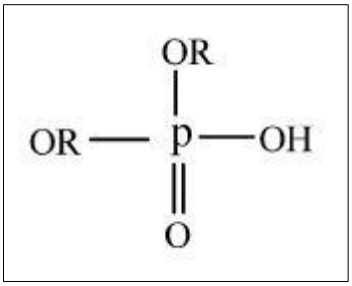

Figure 1.12: Typical structure of phosphate ester [21]

1.7.3 Binder:

Binders are added to the slips to enhance the strength of the green tape for easy handling and storage. The adhesive remains in the tape forming interparticle bridges resulting in a strong adhesion after solvent evaporation. It also improves wetting and delays sedimentation through an increased viscosity. The ideal binder should be compatible with the dispersant act as a lubricant between the particles having no interference with the solvent or trap air, low glass transition temperature (T_g), have an effective binder burnout without residue, be effective at low concentrations, have a high molecular weight that is advantageous to good strength and toughness [20, 21]. The temperature at which the binder changes from a plastic, rubbery state to

a brittle one is referred to as glass transition temperature T_g. Molecular binders of natural or synthetic origin are commonly used for tape casting processes. PVB has been reported for tape casting of different materials such as Al_2O_3, ZrO_2, Al_2O_3/ZrO_2, $Al_2O_3/ZrSiO_4$ and $BaTiO_3$. PVB is prepared by the condensation reaction of an acid-catalyzed butyraldehyde with PVA [21].

Some of the binders used for tape casting are

Methyl cellulose, ethyl cellulose, polyacrylate esters, polymethyl methacrylate, polyethyl methacrylate, polyvinyl alcohol, polyvinyl butyral, polyvinyl chloride and vinyl chloride – acetate.

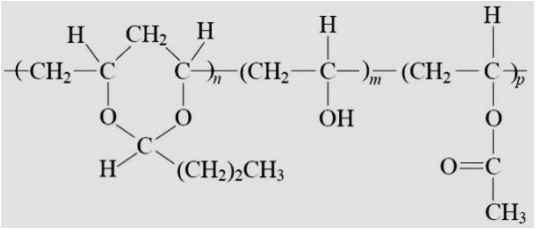

Figure 1.13 Chemical structure of PVB [25]

1.7.4 Plasticizers:

Plasticizers are added to the slip to confer sufficient flexibility to the green tape for easy handling and storage. The most important effect of plasticizer is to reduce the T_g of binder to room temperature or less. This allows working at temperatures higher than T_g and, therefore, leads to better conditions of plasticity [21]. The optimum flexibility is obtained when the corresponding binder/plasticizer system is selected, and the relative concentrations adjusted properly. If plasticizer concentration is increased progressively to enhance the flexibility, the pores will decrease until the pores are full. A further addition results in increasing the interparticle distances and the green density and strength of the tape will decrease.

There are two types of plasticizers:

- **Type-1**
- **Type-2**

Type-1 Plasticizers are used to soften the binder polymer chains allowing them to stretch or deflect under an applied force. These additives can be described as T_g modifiers or binder solvents [21]. The type-1 plasticizer can modify the T_g of a polymer chain by shortening the polymer chain length and by partially dissolving the polymer chain. As the T_g becomes lower, often well below room temperature, the polymer chain better able to stretch or re-orient itself

without fracturing. Excessive use of Type-1 plasticizer would produce a tape that will stretch rather than release from the carrier surface.

Type-2 Plasticizer works as a lubricant in the tape matrix. They work between the polymer chains, not allowing them better mobility within the dry tape, but also preventing some of the cross-linking between chains. The type-2 plasticizer lowers the yield stress and increases strain to failure that prevent cracking in thicker green tapes during drying. The addition of Type-2 plasticizer will increase the tendency of the tape to roll up onto the tape-up reel rather than to release from the carrier [21].

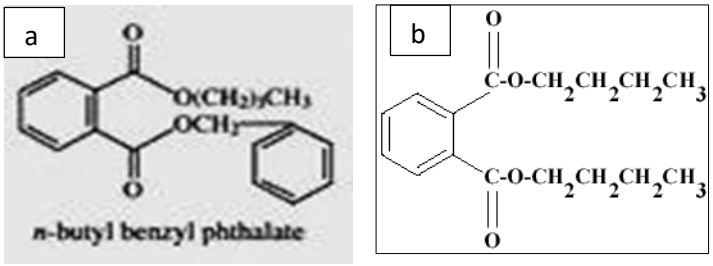

Figure 1.14 Chemical structure of a) BBP and b) DBP [25]

1.7.5 Other additives:

Some other additives are also added to the tape casting slip, those are

1.7.5.1 Homogenizers:

They are added to improve slip homogeneity, preventing skin. Cyclohexane is used for this function.

1.7.5.2 Antifoaming agents:

These prevent foaming during milling time.

In next chapter, a through literature review focused on synthesis and sintering of BZT-BCT, its structural, dielectric and piezoelectric properties will be discussed. Nonaqueous tape casting of different inorganic oxide based materials (specifically $BaTiO_3$ and PZT based materials) would be presented.

References:

[1]. K. Uchino Advanced piezoelectric material: Science and Technology, Wood head Publishing Limited, (2010).

[2]. J. M. Herbert, Ferroelectric Transducers and Sensors, Gordon and Breach, London, (1982).

[3]. B. Jaffe, W. R. Cook Jr., and H. Jaffe, Piezoelectric Ceramics, Academic Press, London, (1971).

[4]. K. Uchino, Ferroelectric devices, Marcel Dekker, (2000).

[5]. A. J. Moulson and J. M. Herbert, Electro ceramics, Materials, Properties, and Applications, Chapman and Hall, London, (1990).

[6]. R. E. Newnham, Properties of materials Anisotropy, Symmetry, Structure, Oxford University Press Inc. New York (2005).

[7]. R. C. Buchanan, ed., Ceramic Materials for Electronics - Processing, Properties and Applications, Marcel Dekker, New York, (1986).

[8]. D. Damjanovic, Rep. Prog. Phys., 61, 1267-324, (1998).

[9]. G. H. Haertling J. Am. Ceram. Soc., 82, 4, 797–818, (1999).

[10]. W. A. Schulze, Ferroelectrics, 87, (1988).

[11]. W. Li, Z. Xu, W. R. Chu, P. Fu, and G. Zang, J. Am. Ceram. Soc.,93, 10, 2942–2944 (2010).

[12]. G. K. Sahoo, Ph.D thesis on "synthesis and characterization of Zr and Ca modified $BaTiO_3$ ferroelectric ceramics", NIT Rourkela, (2014).

[13]. L. Jin, F. Li, S. Zhang, J. Am. Ceram. Soc., 97, 1–27, (2014).

[14]. Y. Saito, H. Takao, T. Tani, T. Nonoyama, K. Takatori, T. Homma, T. Nagaya, and M. Nakamura, Nature, 432, 84, (2004).

[15]. T. Takenaka, K. Maruyama, K. Sakata, J. Appl. Phys., 30, 2236, (1991).

[16]. V. A. Shuvaeva, D. Zekria, A.M. Glazer, Jiang Q, S. M. Weber, P. Bhattacharya, P.A. Thomas, Phys. Rev. B., 71,174114, (2005).

[17]. A. Sen, A. Seal, N. Das, R. Mazumder and H. S. Maiti, International Conference on Smart Materials Structures and Systems, July 28-30, 2005, Bangalore, India.

[18]. J. B. Ihn and F. K. Chang, Structural Health Monitoring, 7, 1, 5–15, (2008).

[19]. James S Reed Principles of ceramics processing, John Wiley and Sons, 2nd edition. (1995).

[20]. R. E. Mistler Tape casting theory and practice, The American Ceramic Society, (2000).

[21]. R. Moreno J. Am. Ceram. Soc. Bull., 71, 1521–1531, (1992).

[22]. R. Moreno J. Am. Ceram. Soc. Bull., 71, 1647–1657, (1992).

[23]. R. Greenwood, E. Roncari, C. Galassi, J. Eur. Ceram Soc., 17, 12, 1393-1401, (1997).

[24]. V. Vinothini, P. Singh and M. Bala subramanian, International Symposium of Research Students on Mat. Sci. Eng. 2004, Chennai, India.

[25]. K. R. Mikeska and W. R. Cannon, Coll. and Sur., 29, 305, (1998).

[26]. D. H. Kim, K. Y. Lim, U. Paik and Y. G. Jung, J. Eur. Ceram Soc., 24, 733–738, (2004).

[27]. J. H. Feng and F. Dogan, J. Am. Ceram. Soc., 83, 7, 1681-86, (2000).

[28]. S. Bhaskarreddy, P. Paramananosingh, J. of Mat. Sci., 37, 929-934, (2002).

[29]. E. Roncari, C. Galassi, F. Craciun, C. Capiani and A. Piancastelli, J. Eur. Ceram. Soc., 21, 409-417, (2001).

[30]. Z. Jingxian, J. Dongliang, L. Weisensel and P.Greil, J. Eur. Ceram Soc., 24, 2259–2265, (2004).

[31]. Y. Qiao, Y. Liu, A. Liu, and Y. Wang, Cer Int., 38, 2319–2324, (2012).

Chapter – 2

Literature review

2.1 BZT-0.5BCT ceramics

Ca, Zr co-doped i.e. (Ba,Ca)(Ti,Zr)O_3 ceramics are used for capacitor application to generate permittivity values as high as ~18000 for Y5V serials [1, 2]. Few work has been performed on the dielectric properties and tunabilities of $(Ba_{1-x}Ca_x)(Zr_yTi_{1-y})O_3$ ceramics and only a few works have focused on the studies of piezoelectric properties of $(Ba_{1-x}Ca_x)(Zr_yTi_{1-y})O_3$ materials [3].

Liu *et al.* [4] designed a non Pb pseudobinary ferroelectric system Ba $(Zr_{0.2}Ti_{0.8})$ O_3-x$(Ba_{0.7}Ca_{0.3})TiO_3$. They investigated a full set of material constant for this compound and interestingly, they found a morphotropic phase boundary (MPB) separating a ferroelectric R (BZT) and T (BCT) phase in the phase diagram (Fig. 2.1a). From the "morphotropic phase boundary" (MPB) composition 50BZT-50BCT exhibited anomaly in all of the properties such as the highest spontaneous polarization, highest remnant polarization, lowest coercive field and highest dielectric permittivity. The range of piezoelectric constant value d_{33} in the 50BZT-50BCT system showed in 560~620 pC/N very much comparable to the commercially available PZTs (Fig. 2.1b).

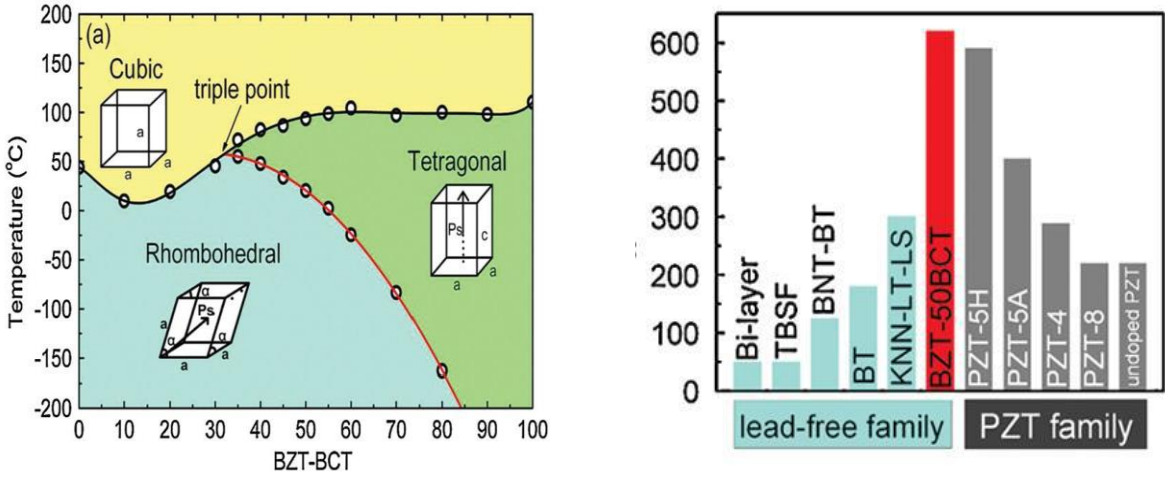

Figure 2.1a) Phase diagram of pseudobinary ferroelectric system Ba(Zr0.2Ti0.8)O3-x(Ba0.7Ca0.3)TiO3 b) Comparison of d_{33} among 50BZT-50BCT and other non-Pbpiezoelectrics and PZT family [4]

Xue *et al.* [5] determined the full set of elastic, dielectric and piezoelectric properties for the BZT-0.5BCT composition prepared by resonance method. This method yielded the d_{33} value of 546 pC/N and a g_{33} value of 15.3 x 10^{-3}Vm/N, elastic constants s^E_{33}= 19.7 x 10^{-12} m^2/N and c^E_{33} = 11.3 x 10^{10} N/m^2 and electrochemical coupling factor was obtained to be of the order of K_{33} =

65%. They observed that these values were in close resemblance to the properties of soft PZT materials. They reported that near the MPB composition these properties are highest and deviations from the MPB composition caused a decrease in these values. Even at -50^{o}C they observed a value of 93 pC/N for the piezoelectric coefficient d_{33}.

Wang *et al.* [6] studied the phase transitions in (1-x)($BaZr_{0.2}Ti_{0.8}O_3$)–x($Ba_{0.7}Ca_{0.3}TiO_3$) (BZT-xBCT) (x = 0.46-0.52) ceramics following solid state synthesis method. Mixed oxides were calcined at 1250^{o}C/3h and sintered at 1400^{o}C/3h. XRD analysis shows the relative contents of monoclinic phase in BZT-0.48BCT and BZT-0.5BCT compositions is higher than those in the other compositions. Piezoelectric constant (d_{33}) for the different compositions are shown in Table – 2.1 The d_{33} values of BZT-0.48BCT and BZT-0.5BCT are higher than those in the other compositions, which mean that the higher piezoelectric properties of these compositions may be related to the presence of monoclinic phase.

Table 2.1 shows the piezoelectric constant (d_{33}) for the different compositions

Composition	**d_{33} (pC/N)**
BZT-0.46BCT	~310
BZT-0.48BCT	~460
BZT-0.5BCT	~410
BZT-0.52BCT	~360

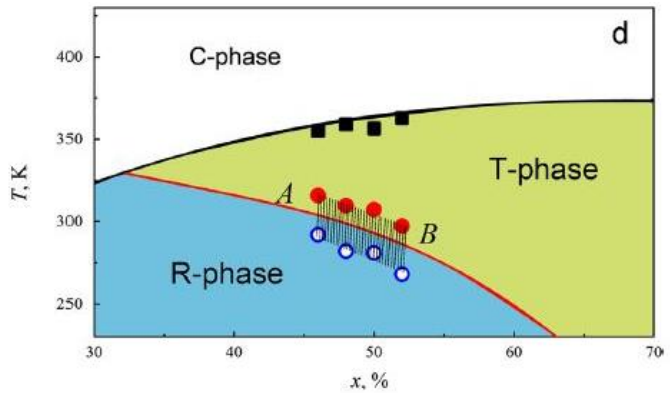

P. Wang *et al*. [7] synthesized lead free ($Ba_{0.85}Ca_{0.15}$)($Ti_{0.9}Zr_{0.1}$)O_3 by conventional mixed oxide method at different calcination (1000^{o}C-1300^{o}C/2h) and sintering temperatures (1500^{o}C-

1550°C/2h). They observed that the BZT-0.5BCT forms MPB between rhombohedral and tetragonal phase at room temperature. It was observed that calcination and sintering temperatures has a significant effect on density and grain size. The BZT-0.5BCT powder calcined at 1300°C and sintered at 1540°C exhibited optimal electrical properties d_{33} = 650pC/N, d_{31} = 74pC/N, k_p = 0.53, k_t = 0.38, k_{31} = 0.309, ${}_sE_{11}$= 14.0 × 10^{-12}m^2/N, ε_r = 4500, tan δ = 0.009, T_c =85°C, P_r = 11.69 μC/cm^2 and E_c = 190V/mm.

Su *et al*. [8] investigated the dependence of poling on piezoelectric properties and electrical properties of BZT-0.5BCT ceramics. The huge piezoelectric coefficient d_{33}~630pC/N and 56% of planar electromechanical coupling factor for BZT-0.5BCT ceramics was obtained by using the optimized poling condition (2.5Ec and 40°C for poling field and temperature, respectively). They also reported that these materials exhibit strong temperature and time dependence, owing to a rather low depolarization temperature (below 80–90°C) and extremely high aging rate (30% and 25% loss for d_{33} and kp, respectively, 10^4 min after poling).

Li *et al*. [9, 10, 11] had reported a low d_{33} of 328pC/ N and high dielectric constant of 4800 in $(Ba_{0.84}Ca_{0.16})(Ti_{0.9}Zr_{0.1})O_3$ ceramics (near around MPB) with a coexistence of rhombohedral and orthorhombic phases. They also reported a d_{33} of 365 pc/N in $(Ba_{0.92}Ca_{0.08})(Ti_{0.95}Zr_{0.05})O_3$ ceramics with an MPB between orthorhombic and tetragonal phases, at the optimal sintering temperature. They also further reported a d_{33} of 387pc/N in $(Ba_{0.99}Ca_{0.01})(Ti_{0.98}Zr_{0.02})O_3$ ceramics with relatively high Curie temperature T_c =115°C. They also modified simultaneously Ca and Zr in $(Ba_{1-x}Ca_x)(Ti_{1-y}Zr_y)O_3$, $(Ba_{0.92}Ca_{0.08})(Ti_{0.95}Zr_{0.05})O_3$, $(Ba_{0.93}Ca_{0.07})(Ti_{0.95}Zr_{0.05})O_3$, $(Ba_{0.99}Ca_{0.01})(Ti_{0.98}Zr_{0.02})O_3$ and found piezoelectric coefficient in between 325-387pC/N at optimal sintering temperature.

Coondoo *et al*. [12] reported the synthesis of 0.5Ba $(Zr_{0.2}Ti_{0.8})O_3$-0.5$(Ba_{0.7}Ca_{0.3})TiO_3$ lead-free ceramic sample by following solid state reaction route, calcining at 1350°C/6h with 1450°C/2h as the sintering temperature. The sample possesses single phase rhombohedral structure at room temperature. They obtained the Curie temperature of the sample at ~97°C with the remnant polarization of 8μC/cm^2 and coercive field of 4 kV/cm. After poling the measured d_{33} value of the sample, is ~350 pC/N with high electromechanical coupling factors kp (44.5%) and kt (41.6%).

Venkata Srinivaspuli *et al*. [13] prepared high dielectric constant and low loss of $x[(BaZr_{0.2}Ti_{0.8})O_3]$-$(1-x)[(Ba_{0.7}Ca_{0.3})TiO_3]$ (x = 0.10, 0.15, 0.20) (BZT–BCT) ceramics by sol-gel method. The phase pure powder was obtained at 800°C for 2 h. The pellets were sintered at 1280°C for 2h in carbolite furnace, and the densities were in the range of 5.32 to 5.49 gm/cc for different compositions. They observed that the average grain size of 0.5 µm to 2µm for different compositions. The average grain size decreases with increase in calcium content. Dielectric constant and Curie temperature (T_c) values decreased with increase in Ca content. They found that d_{33} of the BZT–BCT ceramics is independent of Ca content, and the values lie in between 174pC/N and 177pC/N.

Fei Xiao *et al*. [14] synthesized lead-free $0.5Ba(Zr_xTi_{1-x})O_3$–$0.5(Ba_{0.75}Ca_{0.25})TiO_3$ (x = 0.25, 0.30, 0.35, 0.40) ceramics by conventional solid state method between $BaCO_3$, $CaCO_3$, TiO_2 and ZrO_2. Calcination was performed at 1150^{o}C/3h and sintering was done at 1450^{o}C/2h. With increase in Zr content grain size increased upto x=0.35 for the composition and then slightly decreases. With the increase of zirconium content, the Curie temperature is lowered from 80^0C for x = 0.25 to 25^0C for x=0.4, accompanied by the exchange of corresponding dielectric maximum. For x = 0.35 and x = 0.40 samples the room temperature dielectric constant reached above 10,000 at 1 kHz. Saturation polarization (Ps) of the BZT–BCT ceramics were 14.84, 13.64, 12.9 and 11.16 µC/cm^2 and remnant polarization (Pr) 5.92, 4.52, 2.5 and 1.72 µC/cm^2 for x = 0.25, 0.3, 0.35 and 0.40, respectively.

A Srinivas *et al*. [15] synthesized BZT-0.5BCT by solid state route. Calcination was performed at 1200^{o}C/5h and sintering was done at 1500^{o}C/5h. On XRD analysis of the sintered pellets, it was found that the compound was showing a phase transition between rhombohedral and tetragonal phase. FESEM of the sample showed dense microstructure with a grain size in the range between 8-10 µm. The dielectric constant measured at room temperature is about ~3000. The value of dielectric constant (ε_r) around the Curie temperature (85^{o}C) is about 9700. The decrease in Curie temperature may be caused by the incorporation of stable Zr into the Ti site. Ferroelectric (P–E) and piezoelectric properties recorded for the present system is P_s ~17 µC/cm^2, P_r ~9.1 µC/cm^2, and d_{33} ~400 pC/N.

2.2 Tape casting of $BaTiO_3$ and PZT based system

Mikeska *et al*. [16] reported the tape casting of $BaTiO_3$ (25.0 and 50.0 vol.% solid loading) powder dispersed in MEK (methyl ethyl ketone) – EtOH (ethanol). The objective of the study was to enhance the consistency of tape casting slurry and sintered bodies. Phosphate ester was used as deflocculant. The effectiveness of phosphate ester dispersion was examined by rheological, adsorption, conductivity, and electrophoretic mobility. They used conductivity and adsorption study to establish that the mechanism of dispersion stability is a blend of electrostatic and steric phenomena.

Vinothini *et al*. [17] reported the dispersion of barium titanate nanopowder of average particle size ~ 30 nm. The dispersion of $BaTiO_3$ has been studied using sedimentation experiments in different solvent systems (toluene-ethanol, methyl ethyl ketone-ethanol, xylene-ethanol) along with triton x-100, phosphate ester as dispersants. The author observed that in all solvent systems, phosphate ester undergoes better dispersion (electrostatic repulsion mechanism) when compared with triton x-100 (steric mechanism). They also reported that for better dispersion, the powder suspension should have longer settling time with higher sediment density. The ideal concentration of dispersant was determined from the minimum in slip viscosity. Polyvinyl butyral was used as a binder. The green tape fabricated using xylene-ethanol solvent system with phosphate ester dispersant gives better tapes than other systems.

Chun *et al*. [18] studied different solvent (1-methoxy-2-propanol and ethanol) and different types of a phosphate ester (mono-alkyl, di-alkyl and ethoxy types) for dispersion of nano-sized $BaTiO_3$ powders. They observed 1-methoxy-2-propanol was better solvent than ethanol for dispersion of nano powder. Among the phosphate esters, 2-ethoxy ethyl dihydrogen phosphate esters show the better dispersion of nano $BaTiO_3$ powders. Multilayer ceramic capacitors made of 50 nm suspension contain ultra-thin ceramic layers (2.6-2.9 μm) which shows larger capacitance and superior breakdown voltage than those made of 200 nm $BaTiO_3$ powders.

Boschini *et al*. [19] reported the suspension behavior of barium zirconate in non-aqueous medium. Optimum dispersing conditions are investigated with different solvent systems: trichloroethylene (TCE)-EtOH, MEK-EtOH, methyl isobutyl ketone-MEK-Cyclohexane and pure ethanol. The effect of two different dispersants [phosphate ester (PE) and Hypermer KD-6] was studied for stabilization of the suspensions. Best stabilization was obtained for EtOH with

3wt.% KD-6 and TCE/EtOH with 1wt.% PE solvent-dispersant system of 30 vol.% suspensions. Slip casting of stabilized suspensions were in plaster molds, and green densities higher than 55% of the theoretical density was obtained.

Feng *et al*. [20] studied the effects of xylenes/ethanol solvent mixtures on lanthanum modified lead zirconate titanate (PLZT) by measuring sediment height and viscosity experiments. They found that well-dispersed colloidal suspensions could be prepared in xylene-rich (80/20) solvents with a minimum amount of menhaden fish oil as a dispersant. It was reported that adsorption of dispersant on particle surface strongly depends on the xylenes/ethanol ratio. The solubility of other organic additives, such as a binder, was also important when selecting a xylene/ethanol ratio.

Ronacari *et al*. [21] reported preparation of PZT based suspensions in an azeotropic mixture of MEK-EtOH with four different defflocculants (glycerol trioleate, an amine derivative of an oligomeric polyester, phosphate ester and Polyvinylpyrrolidone). By sediment height experiment, the author observed that both phosphate ester and an amine derivative of an oligomeric polyester produce stable suspensions. Viscosity experiment, shows oligomeric polyester produces a more fluid suspension. After thermal treatment, tape prepared with oligomeric polyester got stuck to the support. Whereas tape casted with phosphate ester showed increased density. Tapes with higher green and fired density, good flexibility and no sticking on the support were obtained using phosphate ester (0.5wt. %) with a solid loading of 20.6 vol%.

Gang Jian *et al*. [22] studied the effect of solid content (34–80 wt.%) of tape casting slurry of PZT on ferroelectric and piezoelectric properties of multilayered films. Nonaqueous tape casting technique was used for fabrication of PZT film. It was found that the ball-milling of the PZT powder improved the rheological properties of the slurry. Weak stability of the slurries was observed for high solid contents (>73wt%). Ceramic films prepared from the slurry with solid contents of 73 wt.% had the optimal structure and properties. After poling at 200 °C with an applied field of 1.2 kV/cm, a $d_{33}$of 294 pC/N was achieved.

2.3 Tape casting of other systems

Jingxian *et al*. [23] reported the effect of five dispersants [polycondensed unsaturated fatty acid, castor oil, phosphate ester, PVB (B79), PVB (B98) on TiO_2 slurries. MEK-EtOH was used as a solvent. The dispersion of TiO_2 was examined through ESA (Zeta potential), rheological and FTIR measurements. ESA test demonstrates that the adsorption of PVB79 and phosphate ester

on the particle surface is of a physical and chemical type, respectively. Rheology and sedimentation measurements show that PVB79 is the best dispersant. FTIR study reveals the adsorption of all dispersants on the powder surface. After the addition of binder (PVB79), phosphate ester produces a more fluid suspension than PVB79 and PVB98. They found that a mixture of phosphate ester and PVB79 could produce better dispersed slurries.

Wang *et al*. [24] studied the preparation of $Ba_{0.6}Sr_{0.4}TiO_3$-MgO suspensions in different solvent systems (azeotropic mixture of toluene–ethanol, methyl ethyl ketone (MEK)–ethanol and zeotropic mixture of xylene–ethanol). They used B_2O_3 and Li_2CO_3 as a sintering aid in the powder mixture. Sedimentation test and rheological measurements were conducted to study the effect of the solvent mixture. While slurries prepared with the MEK–ethanol blend were more stable, exhibiting almost Newtonian behavior and significantly lower viscosity. They found that the formation of gel structure caused by the reaction between hydroxyl group of PVB and dissociated borate in the slurries was suppressed because of the good solubility of PVB and bad dissociation of borate ions in MEK, which make it possible to prepare stable tape casting slurries and to obtain homogeneous and relatively dense green tapes.

Raeder *et al*. [25] studied the dispersion of fully yttria stabilized zirconia in MEK -EtOH azeotropic mixture. They found that there are factors other than surface area and particle size affects the dispersion of the powder. One such important factor is the presence of impurities at the surface of particles. They observed that only three dispersants are efficient [Hypermer KD 1, Polyvinylpyrrolidone (PVP) and a phosphate ester] out of the eleven. PVP shows the less dispersing effect that KD1 and PE. The use of PE as a dispersant possibly leaves traces of phosphorous on the sintered substrate, but this does not impair the oxygen ion conductivity. It was found that the addition of binder and plasticizers to the tape casting slurry did not cause any agglomeration.

Qiao *et al*. [26] studied the non-aqueous tape casting for producing boron carbide green sheet. They used ethanol as a solvent for tape casting. Castor oil, single-oleic acid glycerol, polyvinyl butyral and di-n-butyl phthalate have been used as a dispersant, wetting agents, binder, and a plasticizer, respectively. They also studied the effects of drying condition, milling time and binding systems on the green sheet density and tensile strength. They able to prepare a slurry of 47 at.% of solid loading with particles size of 3.5 μm. The green sheet with high quality can be

attained by the mixing of three-stage milling and drying at room temperature without air convection.

Mukherjee *et al*. [27] reported the role of dispersant and particle size of the powder on the slurry rheology and the corresponding effect on the green as well as on sintered densities of tape cast YSZ. Two common dispersants menhaden fish oil (MFO) and phosphate ester (PE) were used in conjunction with YSZ powders of different particle sizes. It was found that PE is a much better dispersant than MFO, and the best dispersion is obtained with finer (0.18μm)YSZ powder.

Seal *et al*. [28] reported that Pseudoplasticity and viscosity of slurries are two important characteristics that are always to be monitored to get good and reproducible tape-cast samples. The authors observed that ambient temperature has a significant effect on the viscosity and shear rate exponent of a tape casting slurry. They found that the dispersant and plasticizer had important roles to modify the viscosity and shear rate exponent of a tape casting slurry, the binder plays the key role to exhibit the temperature dependence of viscosity and shear rate exponent of the tape casting slurry.

2.4 Tape casting using PVB as dispersant

Tseng *et al*. [29] studied the effect of polyvinyl butyral (PVB) (dispersant) concentration (0.5–5 wt.% of the solids) on the rheological behaviour of barium titanate ($BaTiO_3$) in ethanol–isopropanol mixture at constant solids loading (30 vol.%). They also compared the flow property of $BaTiO_3$ suspension prepared using a commercially available polymeric surfactant KD-6.The PVB acted as dispersant for the $BaTiO_3$ suspension at low concentration levels (PVB 1 wt.%), while it changed to a binder role for higher addition (>2 wt.%) with markedly increased viscosity.They found that a well-stabilized suspension structure is attainable with the PVB addition.

Bhattacharjee *et al*. [30] used PVB as a dispersant for $BaTiO_3$ in the toluene-methanol system, and its efficiency was evaluated by measuring zeta potential and by the rheological study. They observed that the addition of only 1.6 vol% low molecular weight (50,000) PVB was effective in making a well-dispersed suspension. But a small concentration (0.6 vol%) of high molecular weight (2,00,000) PVB is sufficient to stabilize the suspension due to a long chain length of the polymer, which enhances steric stabilization. The adsorption isotherm curve also indicates that the monolayer coverage is complete at 1.6 vol% of the polymer. Better dispersion is obtained by using the reverse azeotropic composition of toluene-methanol (72.4:27.6) than in azeotropic

composition, but the slurries cast with this composition show strong adherence to the glass surface.

2.5 Aqueous slurry processing of BZT-0.5BCT

Ferreira *et al*. [31] studied the long-term stability of aqueous suspensions of BZT-0.5BCT. The effects of aging time on pH and on the leaching extents of Ba, Zr and Ca elements were systematically investigated for the non-treated and surface treated particles against hydrolysis. The efficiency of the dispersants was evaluated by sedimentation tests using suspensions containing 5 wt.% of BZT-0.5BCT powder and a fixed added amount (0.5 wt.%, relative to dry mass of solids) of different dispersant (dolapix, dispex A40, Duramax D-3005). BZT-0.5BCT powder were surface treated by using 2wt.% aqueous solutions of aluminium-hydrogen phosphate, $Al(H_2PO_4)_3$. He observed that Ba^{2+}, Zr^{2+} and Ca^{2+} ions are leaching into aqueous media, and the surface treatment with $Al(H_2PO_4)_3$ reduces hydrolysis and leaching of ionic species into the aqueous media. The rheological analysis of colloidal suspensions revealed that an addition of 0.5 wt.% Dispex A40 enabled achieving optimal dispersion. They showed a method of protecting lead-free BZT-0.5BCT powders against hydrolysis and also revealed how aqueous suspensions with long-term colloidal stability and high solid loadings can be prepared.

Summary of literature review and scope of the work

- The newly discovered BZT- 0.5BCT have attracted considerable attention due to its excellent dielectric and piezoelectric properties. The electrical properties of BZT-0.5BCT solid solutions have been studied extensively; however most of the work focuses on the nature of phase transition, structure, powder synthesis, effect of processing conditions on dielectric and piezoelectric properties and the temperature dependence of the dielectric and piezoelectric properties.
- Multilayered structure (alternate layers of piezoelectric wafers and electrodes) is preferred in most of the actuator applications so that excitation can be done at a low voltage. The applications in SHM often involve piezoelectric ceramics in the form of wafers/substrates that are mainly produced from tape casting. Knowledgebase for making thin individual substrate is also crucial.
- Tape casting is based on the nonaqueous based system, but recently the aqueous based system has gained some importance. Nonaqueous tape casting is fast and easy to fabricate tape, but organic solvents are costly.

- Aqueous tape casting is low cost but major difficulties in drying. In achieving uniform, dense, dimensionally accurate ceramic sheets, the colloidal processing of tape casting slurry is the critical step. Success in tape casting with the required reproducibility and consistency depends upon the degree of dispersion. Recently, stability of BZT-0.5BCT aqueous suspensions was studied in the presence of different dispersants (dolapix, dispex A40, Duramax D-3005), and they observed that Ba^{2+} and Ca^{2+} ions were leaching in aqueous media. It is obvious that BZT-0.5BCT based piezoelectric ceramics device fabricated using aqueous tape casting may have inferior final property.
- Many reports are available on tape casting and rheological study of PZT, PLZT, and $BaTiO_3$. However, there are only a few studies on their electrical properties and, in particular, their piezoelectric properties.
- There are no reports available on the fabrication of BZT-0.5BCT wafers/substrate by nonaqueous tape casting, their densification, and electrical characterization.
- There are very few dispersants available for non-aqueous based tape casting such as Menhaden fish oil, Triton-X 100 and Phosphate ester.
- There are few reports available which tells us that, dispersion of $BaTiO_3$ will be effective if a combination of MEK-EtOH and phosphate ester were used as solvent and dispersant.
- It will be interesting to study how dispersant and binder influence the rheological behavior of BZT-0.5BCT in a non-aqueous medium, castability of slurry, densification and final dielectric and piezoelectric properties.

OBJECTIVES

- The primary objective of the present thesis is to develop a dense warpage free BZT-0.5BCT wafer/substrate with suitable dielectric and piezoelectric property.
- To achieve that goal the effect of dispersant and binder content on the slurry rheology, the properties of tape cast BZT-0.5BCT layers, its densification and dielectric and piezoelectric properties were investigated.

ORGANIZATION OF THE THESIS

The thesis has been divided into five chapters:

Chapter–I Present a brief introduction on basics of ferroelectric, piezoelectric properties, different mechanism for improvement of mechanical properties and important lead-based and lead-free ferroelectric materials

Chapter–II Deals with the detailed literature review of structural, dielectric and piezoelectric properties of BZT-0.5BCT. Synthesis of BZT-0.5BCT by a different method and its sintering also reviewed in details.

Chapter–III Deal with the detail experimental process related to this research work.

Chapter–IV Describes the results and discussion, which has been divided into three sections, where,

- **Section I** Describes the preparation of BZT-0.5BCT powder, densification and electrical characterization in pellet form.
- **Section II** Describes the fabrication of BZT-0.5BCT substrate/wafer by varying dispersant (phosphate ester) and binder (PVB) content. Effect of binder burns out, sintering temperature on densification, dielectric and piezoelectric properties was studied.
- **Section III** Describes the fabrication of BZT-0.5BCT substrate/wafer using PVB as a dispersant as well as a binder. Density, microstructure, dielectric and piezoelectric properties were compared with the substrate prepared using phosphate ester as a dispersant.

Chapter–V Contains the concluding remarks and the scope of future work.

References

[1]. D. F. K. Hennings, H. Schreinemacher, J. Eur. Ceram. Soc., 15, 795–800, (1995).

[2]. H. Kishi, Y. Mizuno, H. Chazono, Jpn. J. Appl. Phys., 42,1–15, (2003).

[3]. D. Hennings, H. Schreinemacher, Mat. Res. Bull., 12, 1221-1226, (1977).

[4]. W. Liu and X. Ren, PRL, 103, 257602 (2009).

[5]. D. Xue, Y. Zhou, H. Bao, C. Zhou, J. Gao and X. Ren, J. of Appl. Phys., 109, 054110 (2011).

[6]. W. Wang, W. L. Li, D. Xu, W. P. Cao, Y. F. Hou and W. D. Fei, Ceram, Int., 40, 3, 3933–3937, (2014).

[7]. P. Wang, Y. Xiang Li and Y. Lu, J. Eur. Ceram. Soc., 31, 11, 2005–2012, (2011).

[8]. S. Su, R. Zuo, S. Lu, Z. Xu, X. Wang, L. Li, Current Appl. Phys 11, S120-S130, (2011).

[9]. W. Li, Z. Xu, R. Chu, P. Fu and Gu. Zang, Mat. Sci. and Eng., B 176 65–67, (2011).

[10]. W. Li, Z. Xu, R. Chu, P. Fu and Gu. Zang, J. Am. Ceram. Soc., 93 10, 2942–2944, (2010).

[11]. W. Li, Z. Xu, R. Chu, P. Fu and Gu. Zang, Physica B 405, 4513–4516, (2010).

[12]. I. Coondoo, N. Panwar, H. Amorín, M. Alguero, and A. L. Kolk. J. Appl. Phys. 113, 214107, (2013).

[13]. V. S. Puli, D. K. Pradhan, W. Perez and R. S. Katiyar, J. Phys. and Chem of Sol., 74, 466–475, (2013).

[14]. F. Xiao, W. Ma, Q. Sun, Z. Huan, J, Li and C. Tang, J. Mater. Sci. Mater Electron 10.1007/s10854-013-1176-4

[15]. A Srinivas, R.V.Krishnaiah, V.L.Niranjani, S.V.Kamat, T.Karthik and Saket Asthana Ceram Int., 41, 2, Part A, 1980–1985, (2015).

[16]. K. R. Mikeska and W. R. Cannon Colloids and Surfaces, 29, 305, (1998).

[17]. V. Vinothini, P. Singh and M. Balasubramanian International Symposium of Research Students on Mat. Sci. Eng. 2004, Chennai, India.

[18]. L. W. Chu, K. N. Prakash, Men T. Tsai and N. Lin, J. Eur. Cer. Soc., 28, 1205-1212, (2008).

[19]. F. Boschini, A. Rulmont, R. Cloots and R. Moreno, Ceram Int 35, 1007–1013, (2009).

[20]. J. H. Feng and F. Dogan, J. Am. Ceram. Soc., 83, 7, 1681–1686, (2000).

[21]. E. Roncari, C. Galassi, F. Craciun, C. Capiani and A. Piancastelli, J. Eur. Ceram. Soc., 21 409-417, (2001).

[22]. G. Jian, Q. Hu, S. Lu, D. Zhou and Q. Fu, Processing and Application of ceramics 6, 4, 215-221, (2012).

[23]. Z. Jingxian, J. Dongliang, L. Weisensel and P. Greil, J. Eur. Ceram. Soc., 24, 2259–2265, (2004).

[24]. C. Wang, H. Ji and J. Wang, J Mater Sci 47, 2486–2491, (2012).

[25]. H. Raeder, C. Simon and T. Chartier, J. Eur. Ceram. Soc., 13, 485-491, (1994).

[26]. Y. Qiao, Y. Liu, A. Liu and Y. Wang, Cer. Int. 38, 2319–2324, (2012).

[27]. Amit Mukherjee, B Maiti, A Das Sharma, R. N. Basu and H. S. Maiti, Cer Int., 27, 731-739, (2001).

[28]. A Seal, D. Chattopadhyay, A. Das Sharma, A. Sen and H.S. Maiti, J. Eur. Ceram. Soc., 24, 2275-2283, (2004).

[29]. W. J. Tseng and C. L. Lin, Mater, Let, 57, 223– 228, (2002).

[30]. S Bhattacharjee, M. K. Paria and H. S. Maiti, J. Mater. Sci., 28, 6490-6495, (1993).

[31]. A. Kaushal, S. M. Olhero and J. M. F. Ferreira, J. Mater. Chem. C, 1, 4846-4853, (2013).

Chapter – 3

Experimental Procedure

3.0 Experimental procedure

3.1 Powder Synthesis, sintering, and characterization

In batch formulation, the raw materials (Metal oxide or carbonate) were weighed according to the stoichiometric formula. All raw materials were preserved prior to the batch formulation in a clean, dry and moisture free desiccator. High purity raw materials were used for batch synthesis. For our work, $Ba(Zr_{0.2}Ti_{0.8})O_3$-0.5$(Ba_{0.7}Ca_{0.3})TiO_3$[BZT- 0.5BCT] will be synthesized by solid state mixing method via ball milling.

Different characterization techniques to study the physical properties of the powder and sintered ceramics were also described.

The BZT- 0.5BCT powder was prepared by ball milling method. Reagent grade of barium carbonate [$BaCO_3$ (Sigma-Aldrich, 99%)], calcium carbonate [$CaCO_3$ (Sigma-Aldrich, 99%)], zirconium dioxide [ZrO_2 (Sigma-Aldrich, 99.9%)] and TiO_2 (Sigma-Aldrich, 99.0%) were used as the starting materials. A stoichiometric amount of powders were mixed by ball mill (Fritizsch Pulveriser) for 12h with zirconia ball using isopropyl alcohol as the media. The mixture was dried at 100°C overnight in an oven. The mixture was placed in an alumina crucible, which was subsequently inserted into the furnace and heated in the temperature range of 1000°C - 1200°C, at 3°C/min in air. Figure 3.0.3 shows the flow chart for the preparation of BZT-0.5BCT ceramics.

For preparation of the bulk sample, calcined powders were mixed with 3 wt% PVA solution with the help of mortar and pestle and dried. The dried powders were pressed into cylindrical pellets (12 mm diameter and 1-2 mm thickness) at 350 MPa in a hydraulic press (Carver Inc., USA) with a holding time of 90 seconds. The pressed green compacts were dried in an oven at 100^0C.

The sintering of the green samples was carried out in a furnace with a heating rate of 3^o/min from room temperature to 650^oC with a holding time of one hour for the removal of binder and inorganic matter respectively. The heating was further carried out at the same heating rate to the final sintering temperature (1500^oC) with a holding time of 4 hours followed by the furnace cooling of the samples to room temperature.

The sintered pellets were coated with silver paste on one side of the pellet and kept under air lamp for drying after one side is completely dried off then coating was done at another side.

After the coating was completed both the sides the pellets were loaded in chamber furnace up to 500ºC/20 min and cooled to room temperature.

3.2 Slurry preparation, tape casting, and characterization
Precursor materials for tape casting of BZT-0.5BCT

Suspensions of BZT-0.5BCT were prepared using reagent grade solvents consisting of an azeotropic mixture of methyl ethyl ketone, MEK (MERCK India) and ethanol, EtOH (Bengal Chemicals). In order to see the effect of dispersants on the slurry rheology, green as well as sintered densities of tapes, two most popular commercial dispersants (PE (Emphos PS21-A) and PVB (Hipol B-30, Hindustan Inks and Resins Ltd. Gujrat, India)) were used in tape casting formulations.

For the preparation of tape casting slurry, the binder used was a PVB and the plasticizer was a mixture of polyethylene glycol, PEG (S. D. Fine-Chem Pvt. Ltd) and benzyl butyl phthalate, BBP (Merck India).

3.2.1 Rheological study

The rheological experiments were conducted by using controlled rheometer (VT500 Haake, Germany, equipped with the sensor system SV1) at 25^0C. Shear dependent behavior of the slurry with 19.28 vol% solid loading with different dispersant concentrations are studied under steady shear conditions was evaluated by ascending and descending shear rate from 4.45 to 444.6 1/s in 2 min, and from 444.6 to 4.45 1/s in 2 min, respectively.

For sedimentation experiments, 3.3 Vol% of solid loading with different concentration of dispersants (0.5 - 2 wt% of powder) is ball milled for 4h and carefully transferred to a 10 ml graduated cylinders. Sediment height is measured as a function of time at regular intervals (1h).

3.2.2 Slurry preparation and tape casting of green tapes:

The preparation of the slurry for tape casting is carried out in two stages. In the first stage deagglomeration and dispersion of powder in the solvent with the aid of dispersant and in the second stage binding system consisted of binder and plasticizer, homogenizers were added to the premixed slurry to achieve complete homogeneity. In both the cases, they were ball milled for 24h in polyethylene jar using ZrO_2 balls as grinding media. Then the slip in the polyethylene jar was de-aired with a vacuum pump for 15 min. Then the slurry was cast in a laboratory tape

caster (Haiku Tech Inc USA) with the stationary reservoir. The slip passes through a double blade system assuring a uniform thickness of the tape, whose height can be adjusted by means of micrometer screws. Slips were cast on a Mylar sheet with a glass substrate as support on it. A casting speed of 1.17 mm/s was maintained in all cases and left for drying over night for the solvent evaporation. All the tapes stripped of from the mylar sheet more or less easily after drying, and all are flexible. Square dimensional samples (1cm x 1cm) were cut from the green tapes and firing was done with a heating rate of 20^0C/h up to 650^0C to allow organic burnout process and 200^0C/h up to 1450^0C and 1500^0C with 6h and 4h soaking time respectively.

Typical laboratory tape casting machine

Figure 3.1Tape Caster [Haiku Tech Inc, USA]

Image of the doctor blade

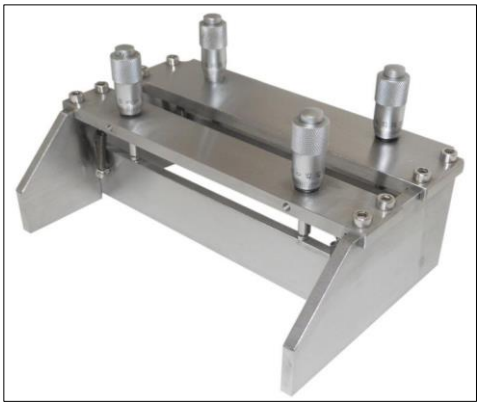

Figure 3.2 Typical doctor blade

Flow chart for fabrication of BZT-0.5BCT tape cast sample

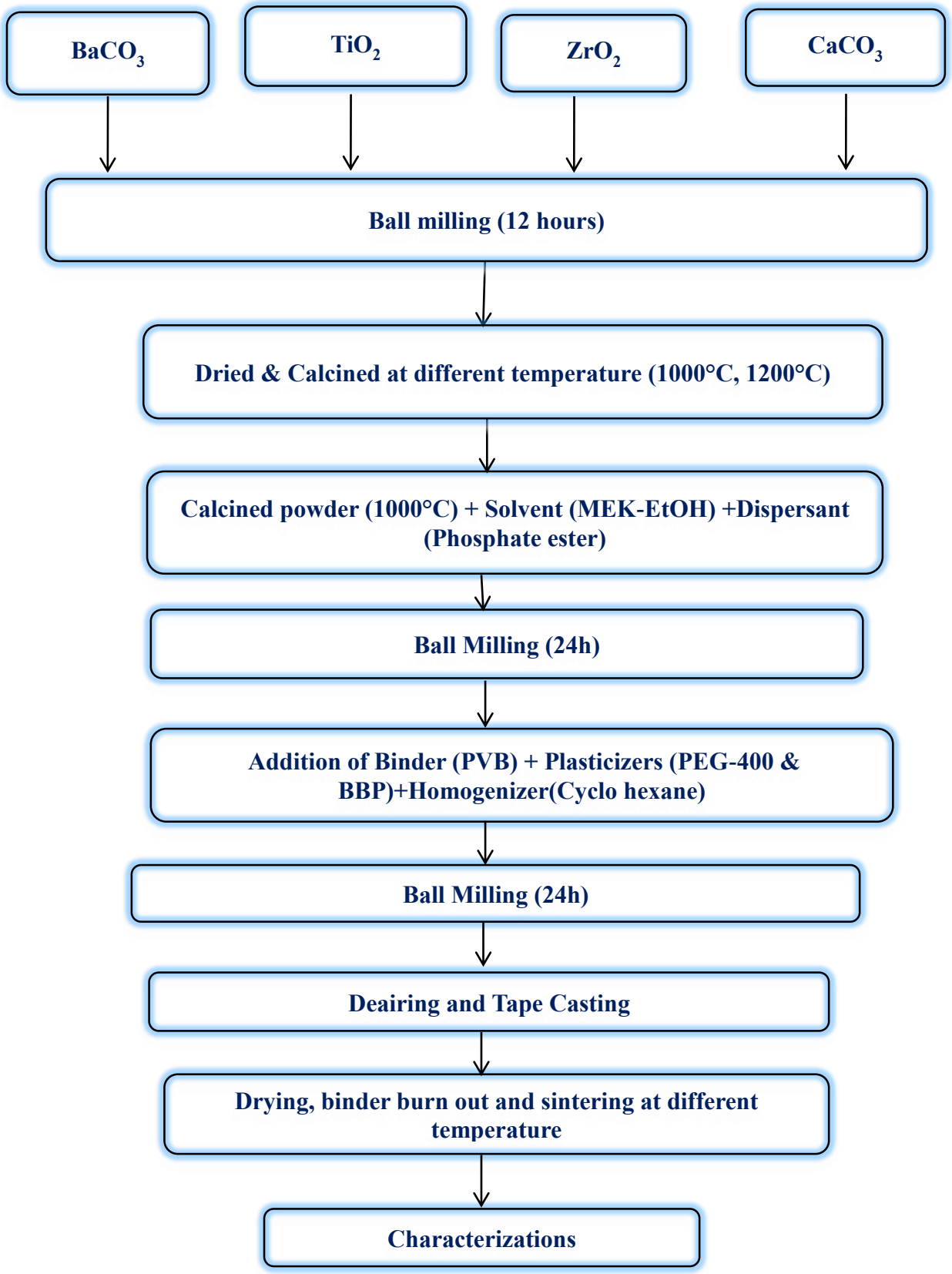

Figure 3.3 Flow chart for fabrication of BZT-0.5BCT tape cast sample

3.2.3 Organic removal and sintering

The dried tapes were cut into square shapes (10-15 mm square) and fired in air at a slow heating rate (20^{o}C/h) from room temperature to 650^{o}C so as to remove the organics. The fired tapes were then sintered at a temperature in the range of 1450^{o}C-1500^{o}C with heating rates between 180^{o}C/h under a top load.

3.3 Characterizations:

3.3.1Thermal analysis

The powder after ball milling was characterized by differential scanning calorimetry (DSC) and thermo gravimetry (TG) using NETZSCH STA (Model No 409C). This technique is excellent for determining the chemical kinetics, enthalpy of transformation, presence and quantity of hydrated water, decomposition behavior, phase transitions, crystallization temperature and formation of products, etc. of precursor powders synthesized through different synthesis techniques. Thermal analysis of precursor powders/green tape has been carried out in an argon atmosphere with the heating rate of 5^{o}C/min from room temperature to 1200^{0}C. When a material undergoes physical or chemical change, it absorbs or releases thermal energy. The temperature differences of the sample with respect to the inert reference material (α-Al_2O_3) during heating or cooling were plotted in a DSC curve.

TGA:

In TGA the sample is heated under nitrogen or argon with constant heat rate while the difference of the mass during this process is measured. A mass loss indicates that a degradation of the measured substance takes place.

DSC:

The DSC can be used to obtain the information on critical thermal points like melting, crystallization, dissociation, enthalpy change specific heat or glass transition temperature of substances. The sample and a reference crucible are heated at constant heat flow. A difference in temperature of both crucibles is caused by the critical thermal points of the sample and can be detected.

3.3.2 Phase analysis

The phase analysis of the raw materials and the sintered samples were determined using the powder X-ray diffraction (Rigaku Japan/Ultima-IV Diffractometer using Cu Kα radiation). X-ray diffraction occurs when there is a constructive interface between the monochromatic x-rays and

the crystalline sample. The crystal structure, crystallinity of the material, crystallite size, chemical analysis, etc. can be known by using this technique. The samples were scanned in the 2θ range 15-80^o at a scan rate of 20^o/min. The generator voltage and current were set at 3.5 kV and 25 mA respectively. The peaks were identified using Philips Xpert high score software.

The sample was placed in a sample holder and was kept for scanning. The diffracted X-rays were detected by an electronic detector placed on the other side of the sample. To get the diffracted beams, the sample was rotated through different Bragg's angles. The goniometer keeps track of the angle (θ), and the detector records the detected X-rays in units of counts/sec and sends this information to the computer. After a scan of the sample, the X-ray intensity (counts/sec) (Y axis) was plotted against the angle theta (2θ)(X-axis). The angle (2θ) of each diffraction peak was then converted to d-spacing, using the Bragg's law;

$$n\lambda = 2d \sin\theta$$

Where, λ = wavelength of x-ray (1.5418 A^o)

n = order of diffraction

3.3.3 Particle size analysis

A laser diffraction method with a multiple scattering techniques has been used to determine the particle size distribution of the powder.Then the experiment was carried out in computer controlled particle size analyzer [ZETA Sizers Nano series (Malvern Instruments Nano ZS)] to find out the particles size distribution.

3.3.4 Density measurement

The bulk density of the pellet samples was measured using Archimedes' principle. The dry weight of the sample was taken and was kept in a beaker filled with kerosene that was placed in a vacuum desiccator for half an hour. The suspended and soaked weight of the samples was taken. The bulk density and apparent porosity of the samples were calculated using the below formulae

$$\text{Bulk Density} = \frac{D}{W - S} * \rho$$

$$\text{Relative Density} = \frac{\text{Bulk Density}}{\text{Theoretical Density}} * 100$$

Where, D= Dry Weight of the sample

S= Suspended Weight of the sample

W= Soaked weight of the sample

ρ = Density of kerosene, 0.81g/cc

The theoretical density of BZT-0.5BCT has been taken as 5.78 gm. /cc in the present study.

For green density measurement of tape substrates, square dimensional samples (1cm x 1cm) were cut from the green tapes, followed by careful measurements of their thickness. The green density of the tapes was then calculated from the weight to volume ratio. To measure the sintered density of the substrates, the above-mentioned pieces of green tapes were fired in air at different temperatures 1450^0C/6h and 1500^0C/4h. Both heating and cooling rates were controlled very carefully to avoid warpage or to crack of the sintered tapes. The densities of the sintered substrate were measured by following above-mentioned technique.

3.3.5 Microstructural Study

Field emission scanning electron microscopy (FESEM) is a typical electron microscope that images formed by simply scanning it with a beam of electrons.The electrons (secondary electrons (SE), back scattered electrons (BSE), characteristic X-rays) interact with the surface atoms which initiate to develop relevant information about the samples microstructure, morphology, pore shape and pore size distribution. The microstructure of the BZT-0.5BCT samples has been elucidated using scanning electron microscope (Nova Nano SEM - 450). Samples were coated with gold in order to avoid charging.

3.3.6 Dielectric and piezoelectric properties

3.3.6.1Dielectric properties measurements

Capacitance and dielectric loss were measured by electroding the samples with silver paste and cured at 500^{o}C for 20 min. Thus, a pellet with two parallel electrodes acts as a single capacitor. Dielectric properties measured using HIOKI 3532-50LCR HI Tester in the frequency range of 100 Hz to 1 MHz. The dielectric properties were also measured as a function of temperature starting from room temperature. The dielectric constant or relative permittivity (ε_r) is the ratio of the permittivity of a substance to the permittivity of free space. The dissipation factor is defined as the tangent of the loss angle (tan δ). It is a measure of the amount of electrical energy that was lost through conduction when a voltage was applied across the piezoelectric material.

The relative permittivity (ε_r) is calculated from the measured values of capacitance and physical dimension of the specimen. The relations are expressed as

$$C = \frac{\varepsilon_o \varepsilon_r A}{t}$$

Where ε_r the relative permittivity of piezoelectric material, ε_o is the permittivity of free space ($8.854*10^{-12}$ F/m), t is the distance between the electrodes (m) and A is the area of the electrodes (m^2).

3.3.6.2 Ferroelectric Measurements: Hysteresis loops

The polarization hysteresis measurement was carried out by an automatic P-E loop tracer (Marine India, Electronics). For these measurements, the thickness of the pellets was reduced to~1mm. The pellets were electroded with silver paste and cured at 500ºC for 20 min. All the measuremenst were carried out at room temperature. The polarization hysteresis measurements based on standard Sawyer Tower circuit. In order to avoid dielectric break down in air, measurement was carried out in silicon oil bath.

3.3.6.3 Poling and piezoelectric measurement

Poling is a process in which a high electric field is applied to the ferroelectric samples to force the domains to reorient along the direction of applied electric field. The poling process of the sintered samples was done using D.C poling instrument in silicone oil at a field of 2 kV/mm for about 20 mins. d_{33} coefficients of the poled samples were measured after 24h of poling with a d_{33} meter (d_{33} Meter, YE2730A, APC International Ltd.). A force of 0.25 N was applied to the sample, and the corresponding d_{33} coefficient is measured.

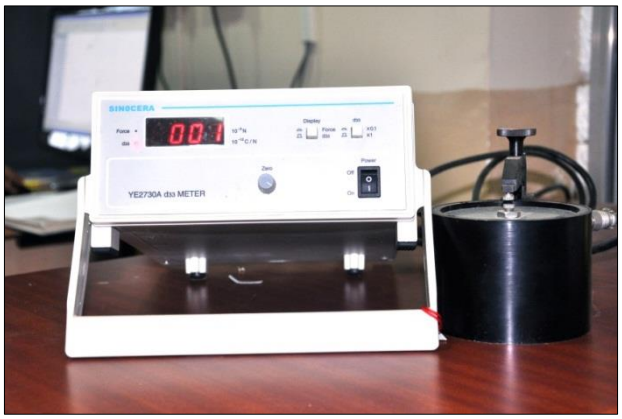

Figure 3.4 d_{33} Meter for piezoelectric measurement

Chapter – 4

Results & Discussions

Section – I Fabrication and characterization of BZT-0.5BCT ceramic

4.1 Introduction

From literature review (chapter 2) it is found that BZT–0.5BCT may be a prospective alternative of lead-based piezoelectric. The present thesis attempts to study the fabrication of dense warpage free BZT-0.5BCT wafer/substrate by tape casting with suitable dielectric and piezoelectric property. Before studying the tape casting of BZT-0.5BCT, it is important to discuss the preparation of BZT-0.5BCT powder and to find out suitable sintering temperature to get best dielectric and piezoelectric property.

The present section deals with the optimization of calcination temperature to get phase pure BZT-0.5BCT fine powder and to study densification behavior and microstructure to get the best dielectric and piezoelectric properties.

4.1.1 BZT- 0.5BCT powder synthesis

4.1.1.1 Thermal analysis of uncalcined powder:

Fig. 4.1.1 shows TG-DSC curves of the uncalcined BZT–0.5BCT powder. The TG plot shows that the overall weight loss is ~18% from room temperature to 1024^{o}C. The total weight loss can be divided into three steps. In the first step (30^{o}C – 650^{o}C), minor weight loss of about ~2% is observed that could be due to the removal of absorbed moisture and isopropyl alcohol. In the same temperature range, the DSC curve shows an endothermic peak, which is correlated to the removal of water of the precursors. In the second and third step, the sample shows a major weight loss of about 16% in the temperature range of 680^{o}C – 1025^{o}C. Two small endothermic peaks can be observed in the corresponding DSC curve at 763^{o}C and 834^{o}C. These endothermic peaks could be attributed to the decomposition of carbonates. The appearance of a broad exothermic peak around 1000-1200^{o}C can be correlated to the reaction among individual oxides and crystallization process of the BZT–0.5BCT powder [1].

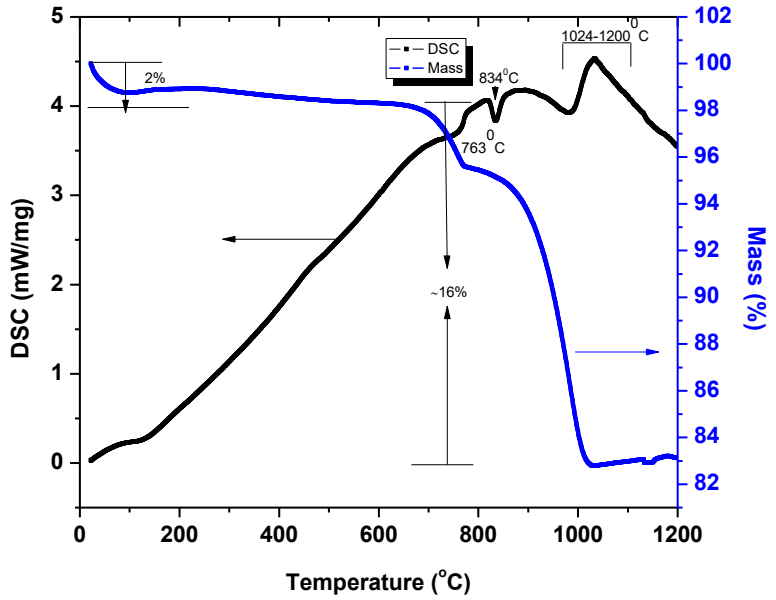

Figure 4.1.1 Thermal analysis of BZT-0.5BCT raw powder

4.1.1.2 Phase analysis of calcined powders:

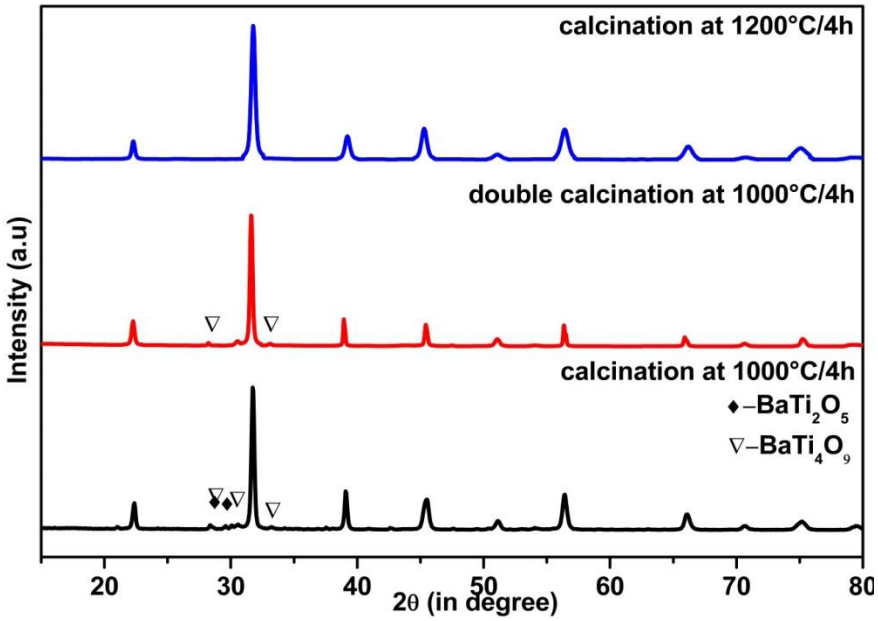

Figure 4.1.2 XRD pattern of BZT-0.5BCT powder calcined at different temperatures

Fig – 4.1.2 shows the XRD patterns of BZT-0.5BCT powder calcined at different temperatures. It is observed that the perovskite phase is formed along with the impurity phases of $BaTi_4O_9$ (JCPDS No-34-0070) and $BaTi_2O_5$ (JCPDS No-70-1188) after calcination at 1000^oC. The complete phase purity was obtained at 1200°C, which is lower than the powder prepared by a conventional method by other researchers [2]. The pure BZT-0.5BCT is showing both tetragonal and rhombohedral (T&R) phase whose XRD data can be matched with the JCPDS No. 89-1428 and 85-1796 respectively [3,4]. The percentage of the perovskite phase was determined by measuring the major XRD peak intensities using the following equation:

$$\% \text{ Perovskite phase} = \left(\frac{I \text{ perovskite}}{I \text{ perovskite} + I \text{ impure phases}}\right) \times 100 \text{ ---------(4.1)}$$

Table 4.1.1 shows the percentage of perovskite phase:

Calcination temperature	Soaking time	Percent Perovskite (%)
1000^0C (C-1)	4h	84.7
Double calcined at 1000^0C (C-2)	4h	96.5
1200^0C (C-3)	4h	100

4.1.1.3 Particle size and morphology of calcined powders

Fig 4.1.3 shows the particle size distribution of BZT-0.5BCT powders calcined at different temperatures. Primarily particle size distribution measured by DLS technique provides the agglomerate size of the powder. The average agglomerate size increased with the increase of calcination temperatures. The average agglomerate size for powders C-1, C-2 and C-3, are 322, 405 and 509 n.m, respectively. Fig 4.1.4 shows the FESEM micrograph of calcined powders. It can be observed that the particles are agglomerated with an irregular to spherical shape particles. The particles size is in the range of 180-500 nm and 270-700 nm for powder C-2 and C-3, respectively. It is also supporting the agglomerate size data received from DLS measurement.

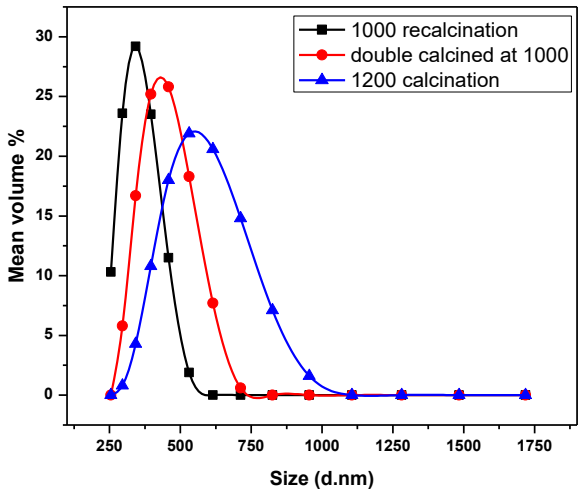

Figure 4.1.3 Particle size analysis of BZT-0.5BCT calcined

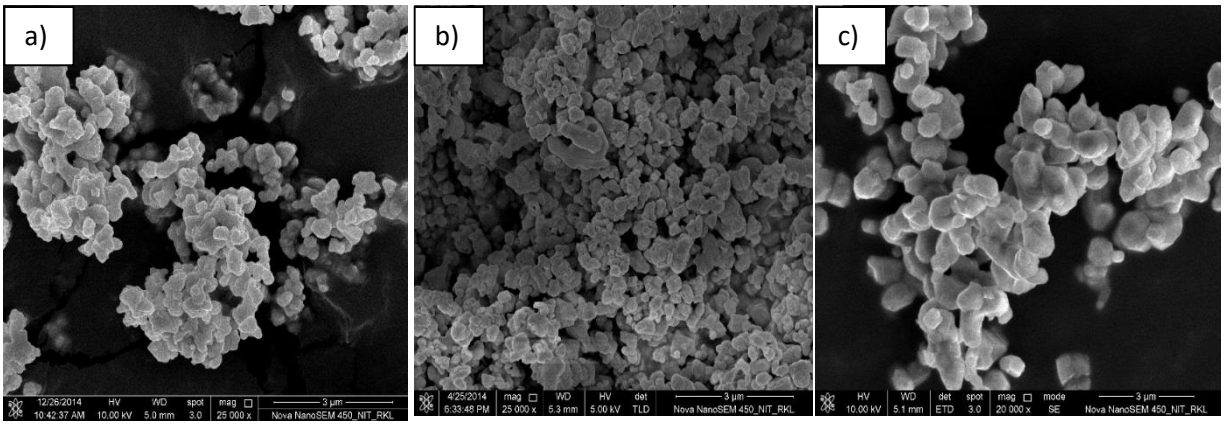

Figure 4.1.4 FESEM Micrographs of BZT-BCT powder a) 1000ºC b) double calcined at 1000^{0}C and c) 1200^{0}C respectively

4.1.1.4 Densification and Microstructure of BZT- 0.5BCT

Table – 4.1.2 shows the relative density of BZT-0.5BCT bulk sample prepared from different temperature calcined powders and sintered at 1500^{O}C/4h. It is evident that the bulk density of the pellets [measured with respect to the true density of BZT-0.5BCT (5.78 g.cm^{-3})] increases marginally with increasing calcination temperature. Fracture surface of the ceramics shows dense microstructure (Fig 4.1.5). P. Wang et al. [2] observed that calcination temperature and sintering temperature have an important effect on the density and microstructure of the final ceramics. They observed that with an increase in calcination temperature from 1000ºC to 1300ºC, the density of the samples improves. They achieved sintered density of 96% and found grain size of 15 µm at a sintering temperature of 1540ºC.

Table 4.1.2 Relative density of BZT-0.5BCT bulk sample

Sample name	Relative density (%)
C-1	94.6
C-2	95.2
C-3	95.6

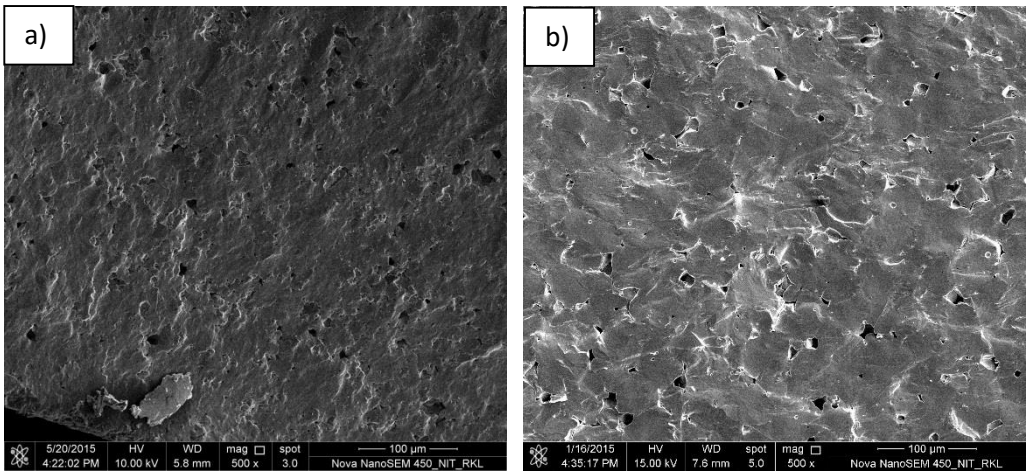

Figure 4.1.5 FESEM Fracture micrograph of BZT-0.5BCT pellet samples a) 1000 Recalcined powder b) 1200 calcined powder sintered at 1500^{0}C/4h

4.1.1.5 Dielectric properties

Fig. 4.1.6 shows the frequency dependence of ε_r and tanδ for BZT–0.5BCT calcined at different temperatures and sintered at 1500^{o}C/4h. It is observed that ε_r improves with increase in calcination temperature. The room temperature value of ε_r at 1 kHz frequency for C-1, C-2, and C-3 samples sintered at 1500^{o}C/4h have found to be 2878, 3098 and 3108, respectively. tanδ in all cases found to be less than 3%. ε_r value of all the BZT–0.5BCT samples decreases with the increase in frequency. Relative permittivity of BZT-0.5BCT ceramics in all compositions in this study are comparable to that of reported in the literature [5-9].

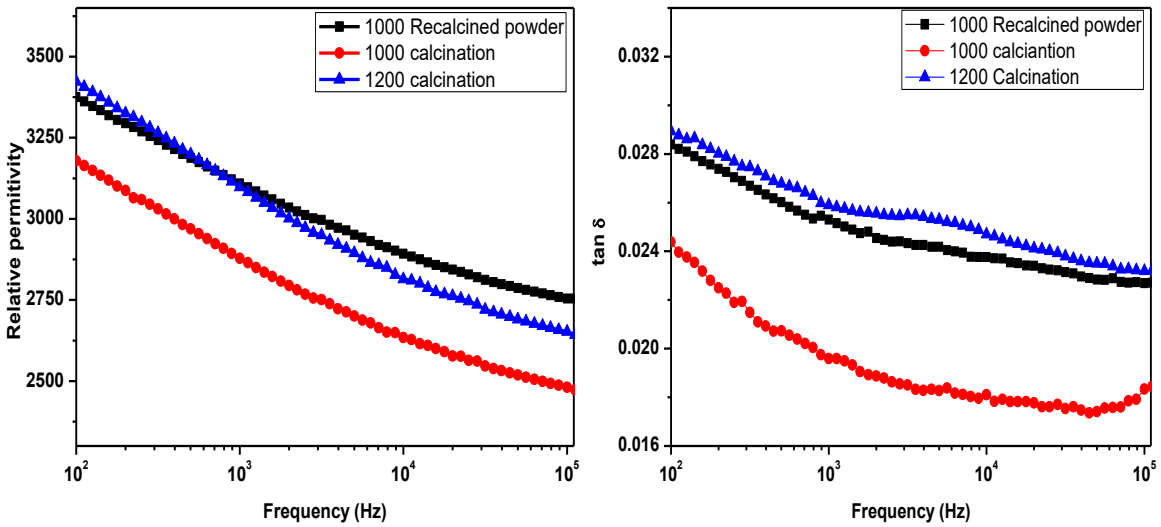

Figure 4.1.6 Variation of dielectric constant of bulk samples sintered at 1500^{0}C/4h

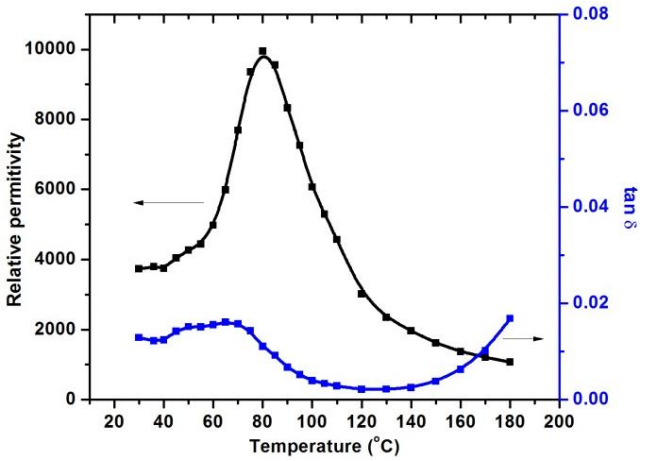

Figure 4.1.7 Variaiton of ε_r and tanδ with temperature

Fig 4.1.7 shows the temperature dependence of ε_r and tan δ for BZT-0.5BCT in the temperature range of 30-180^{o}C. As it can be seen, two peaks are observed, the first peak may be due to polymorphic phase transitions from rhombohedral to tetragonal phase at 35^{o}C. The second peak corresponds to the transition from tetragonal to cubic phase indicating a phase transition from ferroelectric to paraelectric transition at 85^{o}C, which is also in good agreement with earlier reports [2]. Table – 4.1.3 shows the piezoelectric constant (d_{33}) of BZT-0.5BCT ceramics calcined at different temperatures. It can be seen that d_{33} increases with increase in calcination temperature. It may be due to that phase purity of the calcined powder is important to get high d_{33}.

Thus, it can be concluded that the sintered ceramics prepared from double calcined powder (at 1000^{o}C) and 1200^{o}C calcined powder has comparable dielectric and piezoelectric property. The results show that the powder calcined at 1000^{o}C (double calcined) and sintered at 1500°C exhibit good electrical properties: d_{33} = 470 pC/N, ε_r = 3098 and tanδ = 0.0225, respectively. Thus for subsequent studies i.e. rheological behavior and tape casting of BZT-0.5BCT, the powder calcined at 1000^{o}C (double calcined) and 1200^{o}C will be considered.

Table 4.1.3 Variation of piezoelectric coefficient with calcination temperature

Powder calcined at different temperature and sintered at 1500^{o}C/4h	**d_{33} (**pC/N)
	After one day stabilization
C-1	432
C-2	469
C-3	471

Section – II Effect of Dispersant (PE) and binder (PVB) on fabrication of tape and its electrical characterization

4.2 Introduction

In the previous section the preparation of BZT-0.5BCT by solid state mixing method via ball milling was described, where 95% of sintered density could be achieved at 1500^{o}C. The particle size of BZT-0.5BCT can be controlled by tuning the calcination temperature. The dielectric and piezoelectric properties of the sintered ceramics found to be comparable for 1000^{o}C (double calcined) and 1200^{o}C calcined powder though former have a small amount of impurity in the powder.

The applications of piezoelectric ceramics in structural health monitoring (SHM) often required in the form of wafers/substrates that are mainly produced from tape casting. Multilayered structure [14-17] (alternate layers of piezoelectric wafers and electrodes) is preferred in most of the actuator applications so that excitation can be done at a low voltage. Knowledge base for making thin individual substrate is very important (described in Chapter 1). Non-aqueous based tape casting is useful for making thin substrate because of low drying time, easy to fabricate and non-reactivity of oxide particle with solvent (described in Chapter 2). [18-22]. Many reports are available on tape casting and rheological study of PZT, PLZT, and $BaTiO_3$ [23-26]. However, there are only a few studies on their electrical properties and, in particular, their piezoelectric properties [24]. BZT-0.5BCT is a prospective lead-free piezoelectric material. To the best of our knowledge, there are no reports available on the fabrication of BZT-0.5BCT wafers/substrate by tape casting and their electrical characterization.

The present section describes the non-aqueous tape casting of BZT-0.5BCT by studying the effect of dispersant (Phosphate ester) and binder (Poly vinyl Butyral) content on the slurry rheology, the properties of tape cast BZT-0.5BCT layers, its densification, dielectric and piezoelectric properties.

4.2.1 Tape casting of BZT-0.5BCT

In tape casting, homogenous slurry preparation plays a major role in obtaining stable slurry. In general ceramic particles have the tendency to attract each other forming agglomerates due to the presence of vander Waals attractive forces. This could be avoided by the addition of appropriate dispersant/deflocculant which alters the surface charge of the particles or crowded the particle leading to the reduction in the attractive forces and increase the repulsive forces. The best method to know the optimum amount of dispersant is by rheological study. Measurement of

slurry viscosity combined with the sediment height test can be used to judge the relative effectiveness of the dispersed concentration required [18, 19].

4.2.1.1 Effect of dispersant (phosphate ester) on rheological behavior of BZT-0.5BCT slurry:

Fig. 4.2.1a shows the effect of dispersant concentration on the viscosity. It is clear from the figure that the optimal dispersion was obtained at 1wt.% dispersant concentration, which relates to a minimum in viscosity. Sediment height with dispersant concentration also followed the same trend (Fig. 4.2.1b). The sediment height experiment with no.of days (Fig. 4.2.2) indicate that the slurry containing dispersant around the optimum concentration (i.e., 1wt.%) remains almost stable for 4 days (1000^{o}C double calcined), and then they start settling at a faster rate. As expected, the slurry containing higher particle size (1200^{o}C single calcined) settled within 2-3 days and showed higher sediment (settled mass) volume.

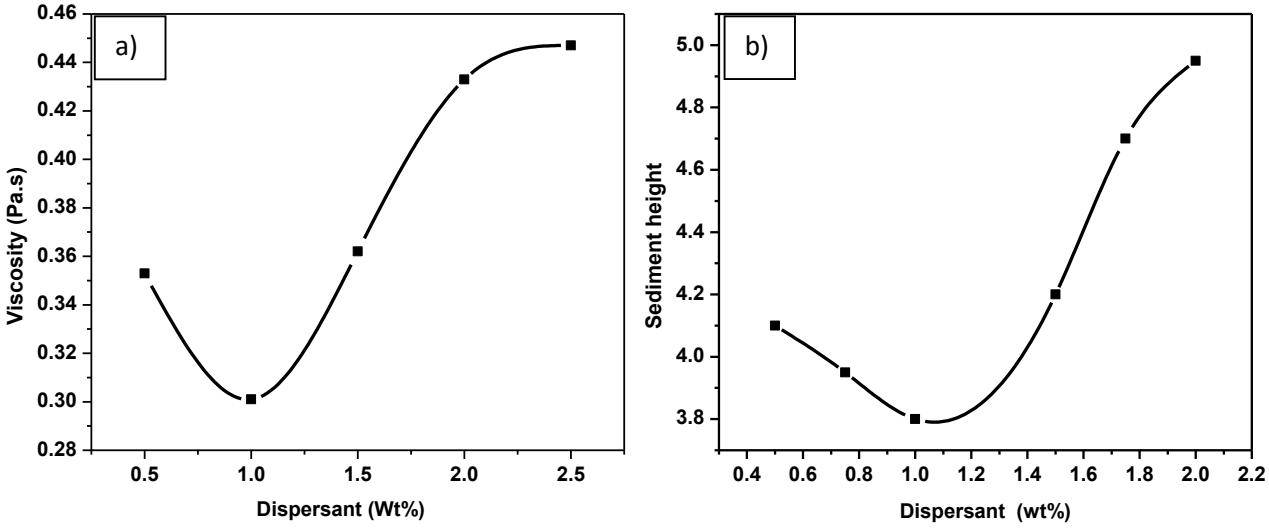

Figure 4.2.1 Effect of dispersant concentration on a) viscosity b) Sediment height

To understand the settling behavior of phosphate ester containing slurries, first we need to consider that phosphate ester acts as an electro-steric [20, 25] dispersant. Phosphate ester ionizes just to a little degree in the MEK/ethanol solvent [26, 31]. In a nonaqueous system the surfactant

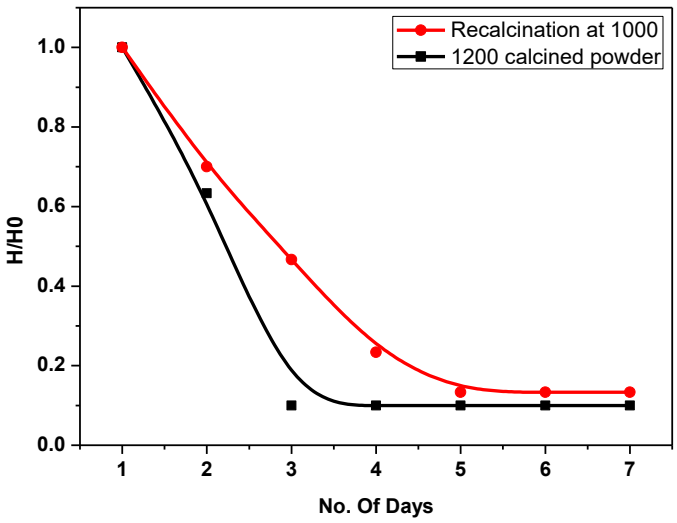

Figure 4.2.2 Effect of particle size on sediment height

adsorbs onto the powder surface as a neutral molecule and charges it positively by exchanging a proton to it. Then certain portion of the anion surfactant desorb, leaving a charged particle that then acts as the electrolyte in the double layer. The steric effect that is caused because of ester helps in the dispersion. Generally, different shapes and sizes of particles were observed in a suspension in which the larger spheres attracted each other when closer due to van der waal forces of attraction. This leads to insufficient space for smaller spheres to fit between them. Depletion flocculation or bridging flocculation takes place when particles are nearer to each other depending on the concentration of the free polymers. When such flocculated particles begin to settle down, it prompts a chain reaction because each particle(s) which drags fluid along with it which then drags on other particles resulting in fast settling of the particles in the slurry. Jingxian et al. [26] and Galassi et al. [27] studied the rheological behavior of TiO_2 and ZrO_2 suspensions using MEK/EtOH as solvent and PE as a dispersant. They observed that the entire powder got settled in half a day and 6.25 days respectively. In the present work, it took four days for the powder to get completely settled. Hence, the high initial viscosity of the slurry could be explained by the insufficient surface coverage of the dispersant molecules on to the BZT-0.5BCT powder particles, resulting in dominated Vander Waals attractive forces. The minimum viscosity obtained at 1wt% dispersant is attributed to the monolayer coverage of dispersant on the particles. Further increase of the dispersant concentration, exceeds the absorption limit and reduces the range of electrical double layer repulsion thus giving rise to an increase in viscosity [18]. Mikeska et al.[18], Galassi et al. [27] and Raeder et al. [28] used MEK/EtOH (solvent) and

Phosphate ester (PE) (dispersant) combination for making $BaTiO_3$, PZT and ZrO_2 suspensions, respectively and found that 0.8, 0.5 and 1.0 wt% of PE is sufficient to get well-dispersed slurries, respectively.

Table 4.2.1 Composition of BZT-0.5BCT tape casting slurry

Ingredient	Function	Weight (%)
BZT-0.5BCT	Ceramic	65-48
Phosphate Ester (Emphos PS21-A)	Dispersant	1.0
Methyl Ethyl Ketone (E. Merck India Ltd.) + Ethanol (Bengal Chemicals & Pharmaceuticals Ltd. India.)	Solvent	25 - 36
Polyvinyl Butyral (Hipol B-30, Hindustan Inks and Resins Ltd. Gujrat, India)	Binder	2.75 - 7
Polyethylene Glycol (S. D. Fine-Chem Pvt. Ltd.)	Plasticizer	3.74 – 5.1
Butyl Benzyl Pthalate (Merck - Schuchardt)	Plasticizer	1.5
Cyclohexanone(S. D. Fine-Chem Pvt. Ltd.)	Homogenizer	1.25

A typical BZT-0.5BCT tape casting slurry was made as per the composition given in Table 4.2.1.

Table 4.2.2 Effect of binder content on solid loading and tape casting of green tape

Composition num	Binder wt%	Solid loading wt %	Remarks
Tape 1	2.75	65	Casting was possible but poor quality tape.
Tape 2	3.0	65	It peeled off from the mylar sheet easily. No visual defect is observed.
Tape 3	3.5	65	It peeled off from the mylar sheet easily. Small binder agglomerates can be observed.

Tape 4	4	60	It peeled off from the mylar sheet easily. No visual defect is observed.
Tape 5	5	56	It peeled off from the mylar sheet easily. No visual defect is observed.
Tape 6	6	52	It peeled off from the mylar sheet easily. No visual defect is observed.
Tape 7	7	44	Casting was possible but poor quality tape

4.2.1.2 Study on rheological behavior of BZT-0.5BCT tape casting slurry

The rheological study plays an important role to understand the slurry processing. Two kinds of study i.e., the effect of low binder content and high binder content on the rheology of the slurry can be observed (Table 4.2.2). In tape casting while passing the blade, the viscosity decreases due to shear forces and immediately the viscosity increases behind the blade. This suppresses the uncontrolled flow and delays sedimentation of the ceramic particles [14].

4.2.1.3 Effect of low binder content on viscosity of slurry:

By considering the above dispersing conditions, the effect of low binder concentration on the viscosity of the slurry was studied. Fig. 4.2.3 shows the effect of shear rate on viscosity as a function of binder concentration. The binder concentration was increased from 2.75 – 3.5 wt%, keeping the solid loading at 65%. Viscosity increases with increase in binder addition, by adding large binder amount more aggregates are generated which hampered the shearing effect there by resulting in increased viscosity [28].

The rheological behavior of the slurry can be described by the power law model (Hershel-Buckey) equation

$$\tau = k\gamma^{n}$$

Where τ is the shear stress, γ is the applied shear rate, k is the consistency factor, and n is the shear rate exponent. The shear rate exponent value $n<1$ is attributed to shear thinning in particle loaded systems and the greater the divergence from Newtonian behavior the lower is the value of n. The slurries with $n>1$ exhibit the shear thickening behavior where the viscosity increases with applied shear stress. This behavior indicates a concentrated suspension with large agglomerates, concentrated and deflocculated slurries [18, 26]. The Non-Newtonian constant has been found to be 0.438, 0.473 and 0.466 for Tape-1, Tape-2, and Tape-3, respectively are shown in Table 4.2.3. This indicates that all the slurries prepared in this study showed Non-Newtonian behavior. Shear-

thinning behavior is generally connected with the slurry structure. At low shear rates, fluid is immobilized in unfilled spaces inside flocs and the floc system. As the shear rate increases, the flocs and floc system break down, the entrapped fluid is discharged, and a more ordered structure is formed in the flow direction [25]. Mukherjee et al. reported that for yttria stabilized zirconia using MEK-EtOH as solvent and Phosphate ester as dispersant the values of n are in the range of 0.91-0.97 [29].

Table 4.2.3 Effect of binder concentration on shear rate exponent

Binder wt%	Shear rate exponent (n)
2.75	0.438
3.0	0.473
3.5	0.466

Table 4.2.4 Characterization of shear thinning behavior of slurry by the ratio of viscosities

Binder wt%	P (ratio of viscosity at1 s^{-1} and 56.4 s^{-1})
2.75	5.61
3.0	5.26
3.5	6.07

From Table–4.2.4 shows the shear thinning (P) characterization of the slurry by the ratio of viscosities at different shear rates. Here in this study the chosen shear rates are 1 s^{-1} and 56.4 s^{-1}. When P = 1, the viscosity is independent of shear rate (Newtonian behavior). When P > 1 the slurry has shear thinning behavior, the bigger is P, the greater is the shear-thinning. The values of 'P' reported in the literature are in the range 5.53-7.90 [30].

Tape 1 could be casted easily when compared with other compositions because of the presence of less binder which made the slurry less viscous when compared to other compositions having same solid loading. We have also observed that with an increase in the binder content the viscosities of slurries increased leading to difficulty in transportation of slurry to the reservoir. However, with an increase in binder amount the removal of tapes from the substrate became

easier with improved handling strength. Fig 4.2.3 shows the visual appearance and micrographs of green tapes. It can be seen that Tape - 1 is having uneven surface through out the length of the tape and while peeling off from the substrate it got cracked. The possible reason for this might be the amount of binder added may not be sufficient to bind individual particles resulting in very less tape strength. Tape 2 is having a uniform surface, and no visual defects can be observed but in Tape-3 some binder agglomerates can be observed.

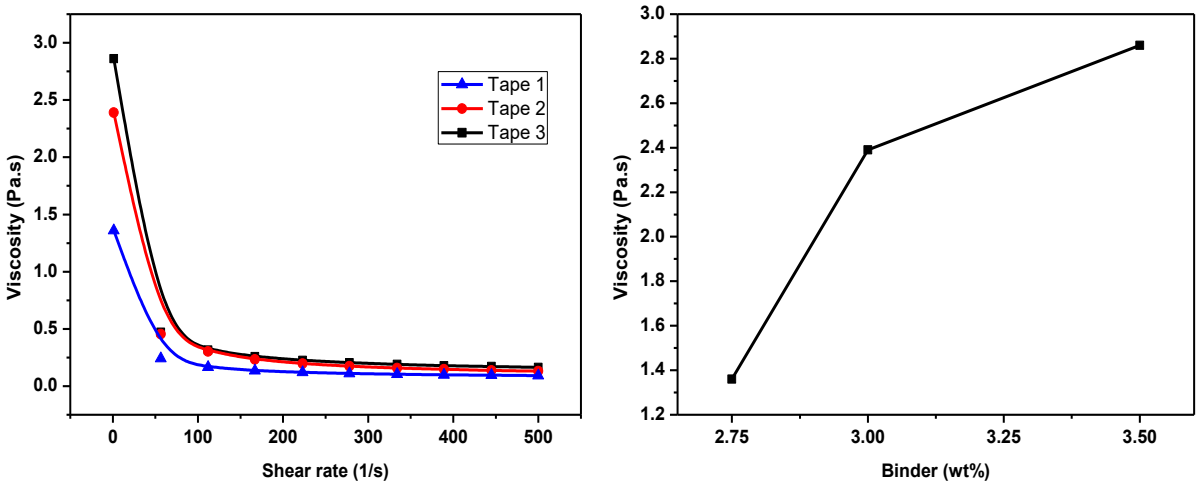

Figure 4.2.3 Effect of low binder content on viscosity of slurry

4.2.1.4 Physical appearance of green tapes

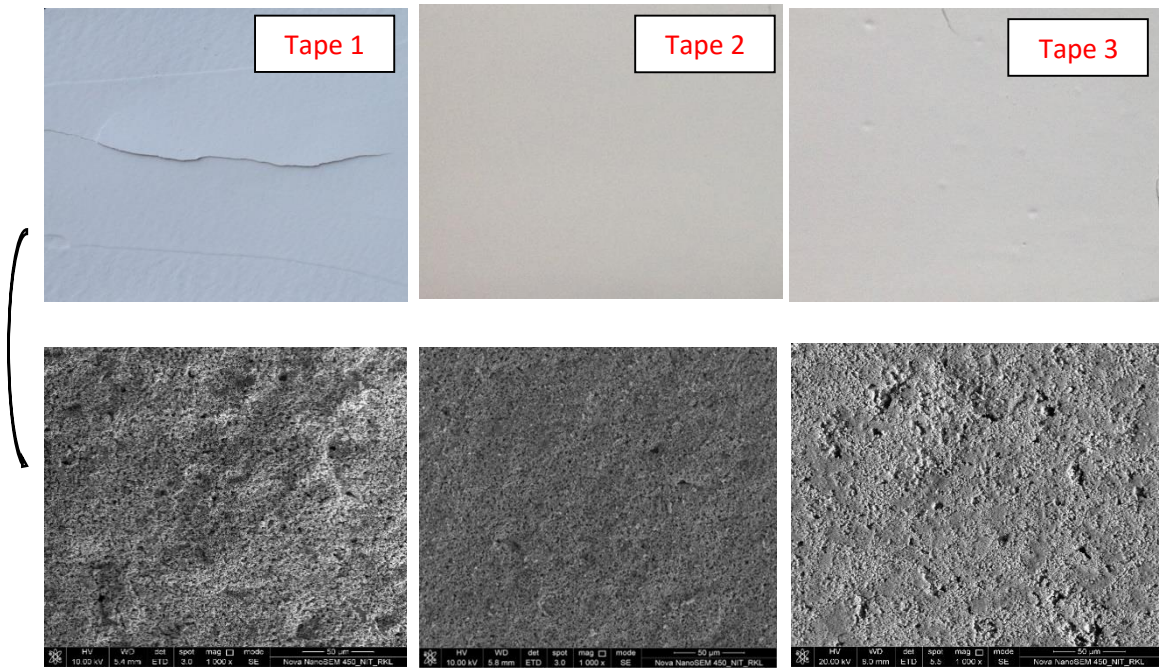

Figure 4.2.4 Visual appearance and micrograph of tape samples with low binder content

4.2.1.5 Effect of high binder on the viscosity of slurry

Fig.4.2.5 shows the effect of high binder content on the viscosity of the slurry. The rheological behavior of these slurries showed pseudo plastic behavior. Though the slurries (4-7 wt%) showed difference in viscosity (1.18-0.69 Pa.s) at low shear rate ($1s^{-1}$), but at high shear rate (500 s^{-1}) the difference is very less (0.0878 – 0.0435 Pa.s) indicating that the slurries are pourable under shear. The reason for decrease in viscosity with increase in binder content (4-7 wt%) is due to addition of more solvent for dissolving the binder, resulting in decrease of solid loading (65-44.0 wt.%). If the solvent were inadequate for dissolving the binder, the sheet would be inhomogeneous, and the larger agglomerations would remain. The agglomerates will lead to the density differences in different parts of the tape [30]. Fig.4.2.6 shows the visual appearance of green tapes after drying. From the image of Tape-7, it can be observed that the tape casted with 7 wt% binder failed immediately after casting. The possible reason for this might be low solid loading. However, the addition of high amount of binder could not bind the individual particles. On the other hand, composition using lower binder content (<7 wt%) casted easily, and no visual defects were observed and peeled off from the mylar substrate very easily.

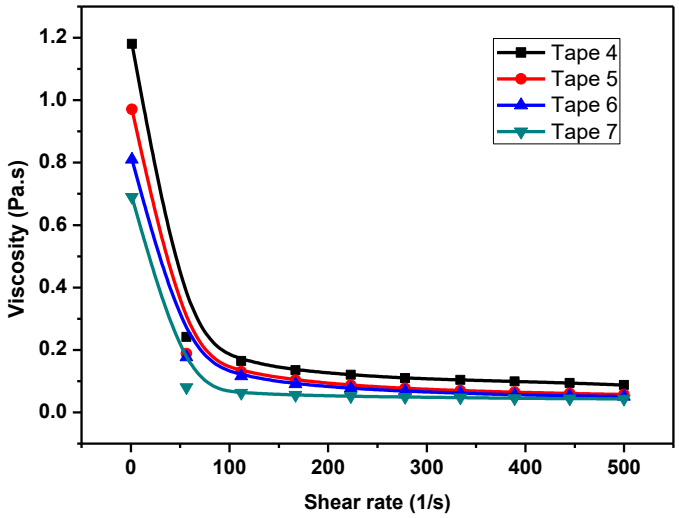

Figure 4.2.5 Effect of binder on the viscosity of slurry

Table 4.2.5 Variation of Shear rate exponent (n) with high binder amount

Binder wt%	Shear rate exponent (n)
4	0.283
5	0.272
6	0.299
7	0.325

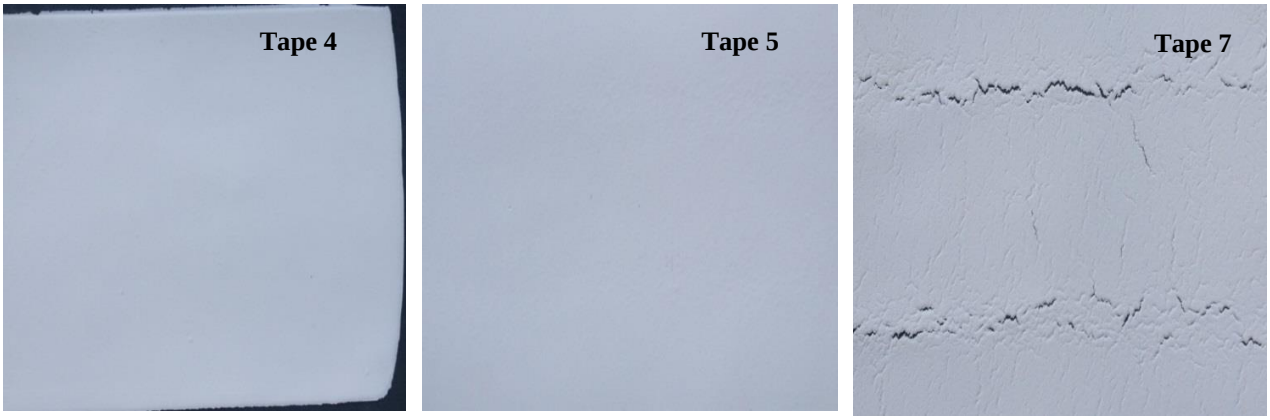

Figure 4.2.6 Visual appearance of green tapes with high binder content

4.2.1.6 Thermal analysis of green tapes:

The thermo gravimetric (TG) analysis of the green tape is shown in Fig.4.2.7. There is a slight decrease in weight from room temperature to 200^{o}C which is caused due to the evaporation of the absorbed water. A sharp weight loss was observed in the temperature range of 200^{o}C to 400^{o}C followed by another weight loss in the temperature range of 600-680^{o}C [31]. With the further increase in temperature beyond 700^{o}C, no major weight loss was observed. The burn out of phosphate ester took place at a low-temperature range i.e. 220-300^{o}C followed by the decomposition of the first plasticizer that arose between 240 and 380^{o}C. That is due to the low molecular weight of BBP compared to PVB [31]. The decomposition of the binder took place in an easier way due to the removal of the organic additives at lower temperature after the elimination of the first plasticizer. The burnout of binder took place in single step until 400^{o}C and thereafter a second step arose in the temperature range of 400-600^{o}C due to the decomposition of residual defloculant and second plasticizer. The weight loss that took place after 600^{o}C was due to the presence of more binder that required a higher temperature for

complete decomposition [31]. The thermal analysis of individual component phosphate ester and PVB was also carried out (Fig 4.2.7(b)). It is observed that the complete dissociation of PVB took place around 500^{o}C and further no weight loss was observed. On the other hand, PE showed rapid weight loss happened around 300^{o}C and a small weight loss is also observed around 850^{o}C. Tseng et al. and Bhattacharjee et al. also reported that complete pyrolysis of ester molecules requires very high temperatures (800^{o}C) [32, 33].

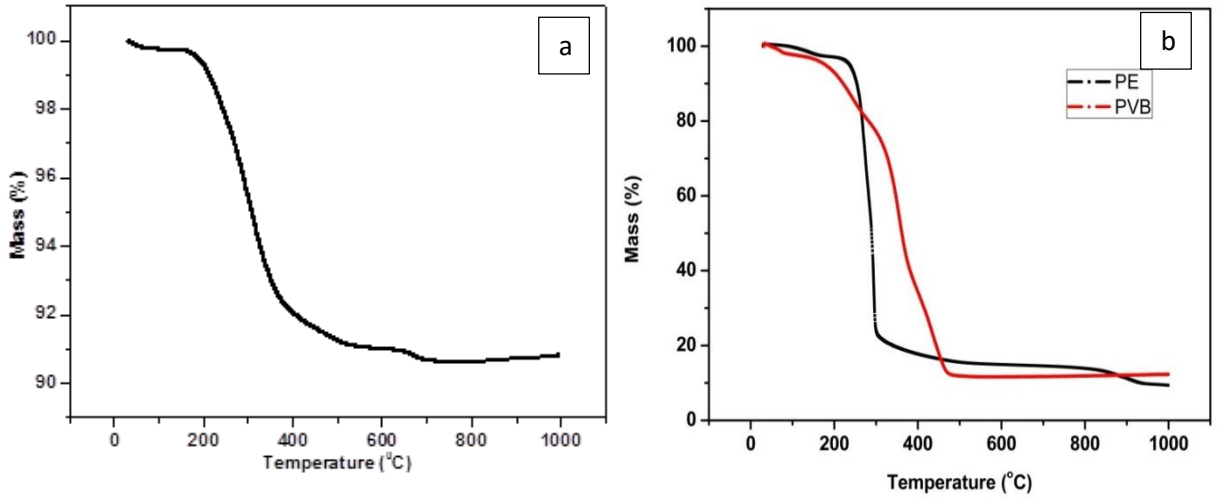

Figure 4.2.7 Thermal analysis of a) green tape b) organic additives

4.2.1.7 Binder burn out/organic removal and sintering of green tapes

Actually, making satisfactory tapes by controlling the slurry rheology [34] does not ensure good quality final substrates/wafers. Some of the problems unique to fabrication of dense, flat BZT-0.5BCT wafers are i) thin tapes easily curl and warp due to differential shrinkage during sintering [34], ii) The binder burn out/organic removal is a critical step which must be accomplished without any disruption of the structure and a very slow heating schedule is necessary iii) tapes often stick to the setter plates and may crack or break during removal. Keeping in view the TG analysis of the green tape and major individual components (PE and PVB) binder burn out/organic removal was carried out in two different temperatures e.g. 650^{o}C and 850^{o}C. Sintering was carried out in two different temperatures e.g. 1450^{o}C and 1500^{o}C. Identification of the different sample mentioned below (Table -4.2.6):

Table 4.2.6 Identification of samples

Sample Index	Binder burn out temperature	Sintering temperature
S1	650	1450
S2	650	1500
S3	850	1450
S4	850	1500

Firing of green tapes is done by applying a load on the samples; this load allows the tape sample not to get warped while sintering. Fully stabilized zirconia substrate was used for firing. Fig 4.2.8 shows the tape samples sintered with varying load. Three different load 0.55, 0.81 and 1.4 gm/cm^2 are used, and the flatness of the substrate was observed. While using 0.55 gm/cm^2 of load warpage is observed on the tape sample. The flat substrate can be found with a top load of ~0.81 gm/cm^2. It is noted that the tape got stuck to the substrate with a load of ~1.4 gm/cm^2. It can be concluded that the 0.81 gm/cm^2 is sufficient to get warpage free substrate.

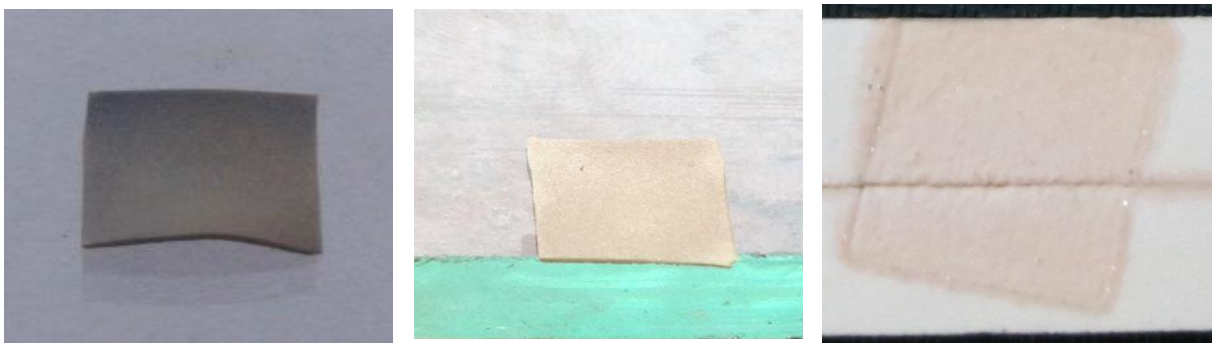

Figure 4.2.8 Visual appearance of wafer/substrate sintered with varying load (a) 0.55 (b) 0.81 and (c) 1.4 gm/cm^2

4.2.1.8 Densification and microstructure of BZT-0.5BCT substrates

Fig 4.2.9 shows the density of green and fired substrate as a function of solid loading of the slurry, binder burn out temperature and sintering temperature. It is observed that with an increase in solid loading the density increases. Further, the density also increases with increase in sintering temperature. Tape-2 sintered at 1500^{o}C shows highest relative density (94%). It is also observed that the sintered density reduces with increase in binder burn out temperature to 850^{o}C. It can be explained by considering that a residual phosphorus-rich layer covers the BZT-0.5BCT particles at high temperature that involves phosphorus diffusion through the particles leads to the formation of a BaO-rich phase [35]. During high-temperature binder burn out for a substantial time (850^{o}C/4h), both the mobility of the P^{5+}cations and the BaO enrichment of this phase

increase. The presence of phosphorus–BaO-rich phase that covers the BZT-0.5BCT particles may act as a diffusion barrier that inhibits mass transport between the adjacent grains and hinders sintering [36]. Probably this phenomenon is less active in case of 650^{o}C binder burn out temperature. From microstructure (Fig. 4.2.10) it is clear that porosity of the substrates decreases with increase in solid loading and sintering temperature. Incidentally, S-4 has smaller grain size (15 μm) (Fig. 4.2.11) compared to S-2 (24 μm) sample (Fig. 4.2.10-2). In the present case residual phosphorous inhibited grain growth. Since no second phase has been detected for samples sintered at 1500^{o}C, it is expected that P^{5+} is incorporated in the BZT-0.5BCT lattice. However, the low solid solubility of P_2O_5 in $BaTiO_3$ was reported [37]. It may be that phosphorous cations are accumulated at the grain boundaries, and high-temperature binder burn out for a substantial time (850^{o}C/4h), generates more amount of phosphorus–BaO-rich phase that inhibits grain growth effectively in S-4 samples (Fig. 4.2.11-b). In the present case, the further systematic study can find out the role of the phosphorous on densification of BZT-0.5BCT.

.

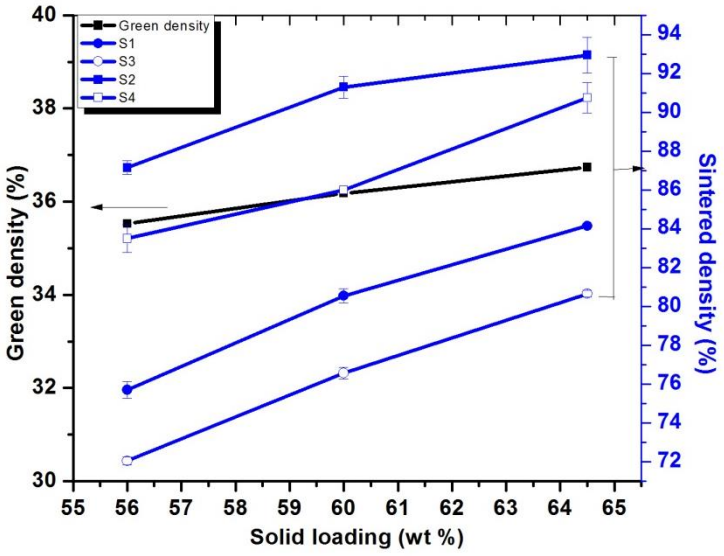

Figure 4.2.9 Shows the green and fired density of substrates

Fig 4.2.10 & 4.2.11 shows the surface and fracture microstructure of tape samples sintered at 1450^{o}C/6h and 1500^{o}C/4h. It can be clearly seen that with the increase in binder content porosity gradually increased and, on the other hand, the porosity decreased (which means that density has increased) with increase in sintering temperature, which is well matched with density data.

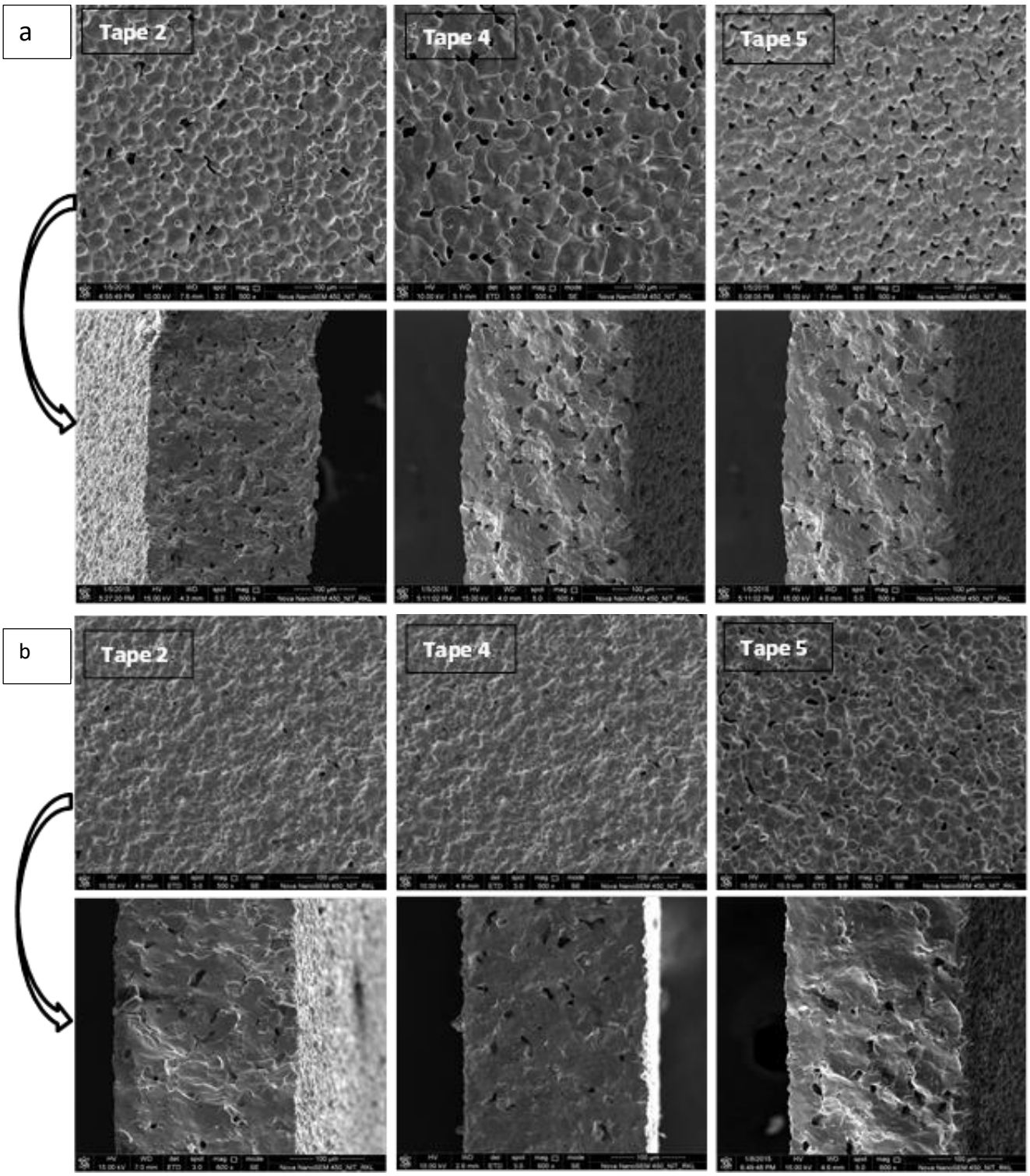

Figure 4.2.10 FESEM Micrograph of a) S1 b) S2

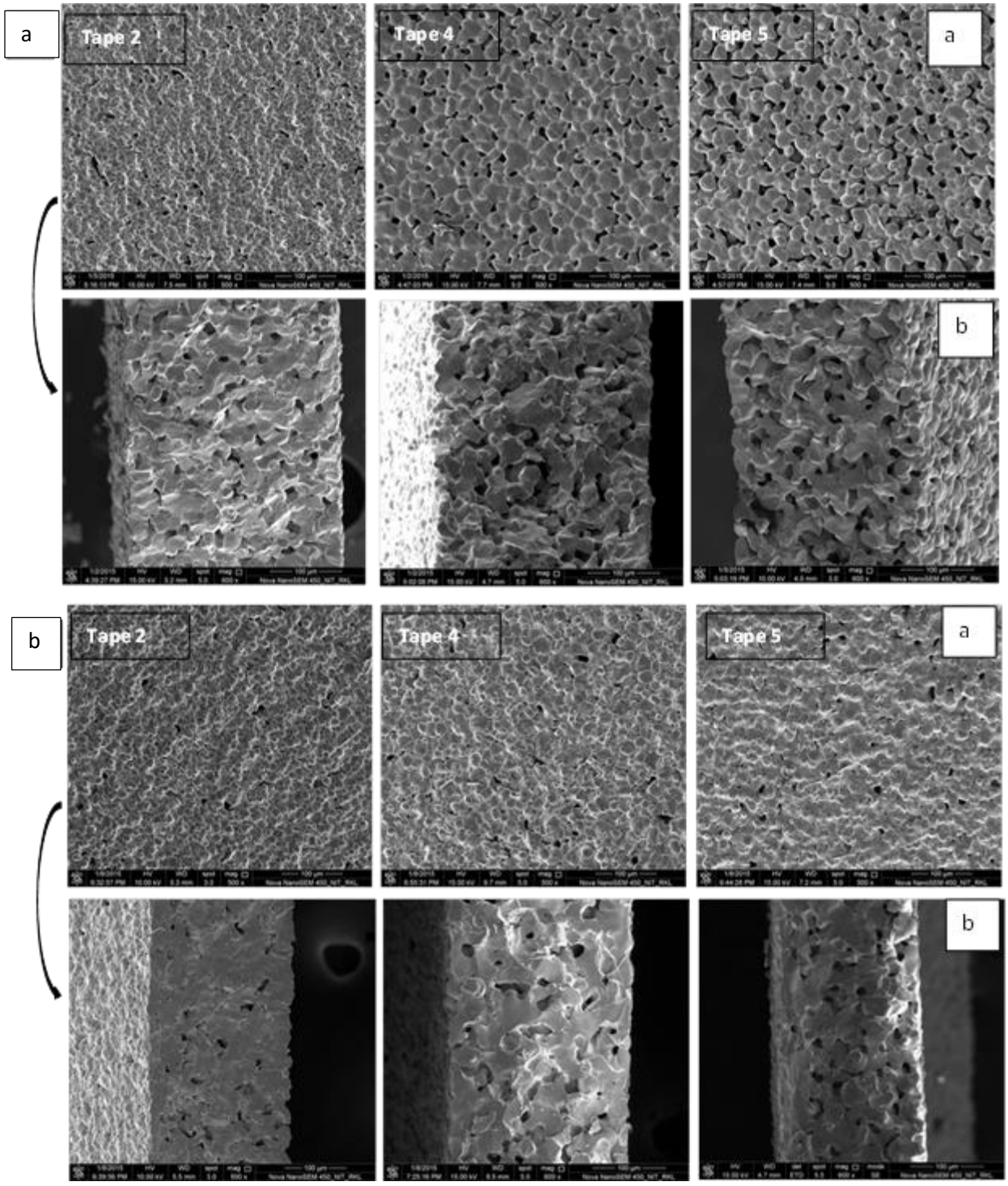

Figure 4.2.11 FESEM Micrograph of a) S3 b) S4

4.2.1.9. Dielectric properties

Figure 4.2.12 and 4.2.13 shows the relative permittivity and loss factor as the function of frequency (100Hz to 1MHz), solid loading and binder burn out temperature for BZT-BCT substrate sintered at 1450°C/6h and 1500°C/4h measured at room temperature. Relative permittivity increased with increasing density and solid loading. Dielectric and piezoelectric properties of the BZT-BCT wafer are also dependent on the sintering temperature. The permittivity for Tape- 2 sample (1710.2 and tanδ 2.5% at 1kHz) is higher than other samples, which may be attributed to higher relative density (low porosity), since, in general, porosity lowers the permittivity. This permittivity is lower compared to bulk ceramics (discussed in section 1). However, it is at par with BCZT thick films fabricated via screen printing by Bai et al. [38]. Dielectric loss is reduced with an increase in sintering temperature to 1500^{o}C. Also, the dielectric loss tends to rise without showing a peak at low frequency. This is a signature of Maxwell–Wagner type relaxation [39, 40] which is the consequence of charge accumulation at the discontinuities/grain boundaries within the dielectrics. Inferior dielectric property of 850^{o}C binder burn out sample may be attributed to the lower density and higher concentration of phosphorous-rich grain boundary phase. Smaller grain size in these samples is also supporting

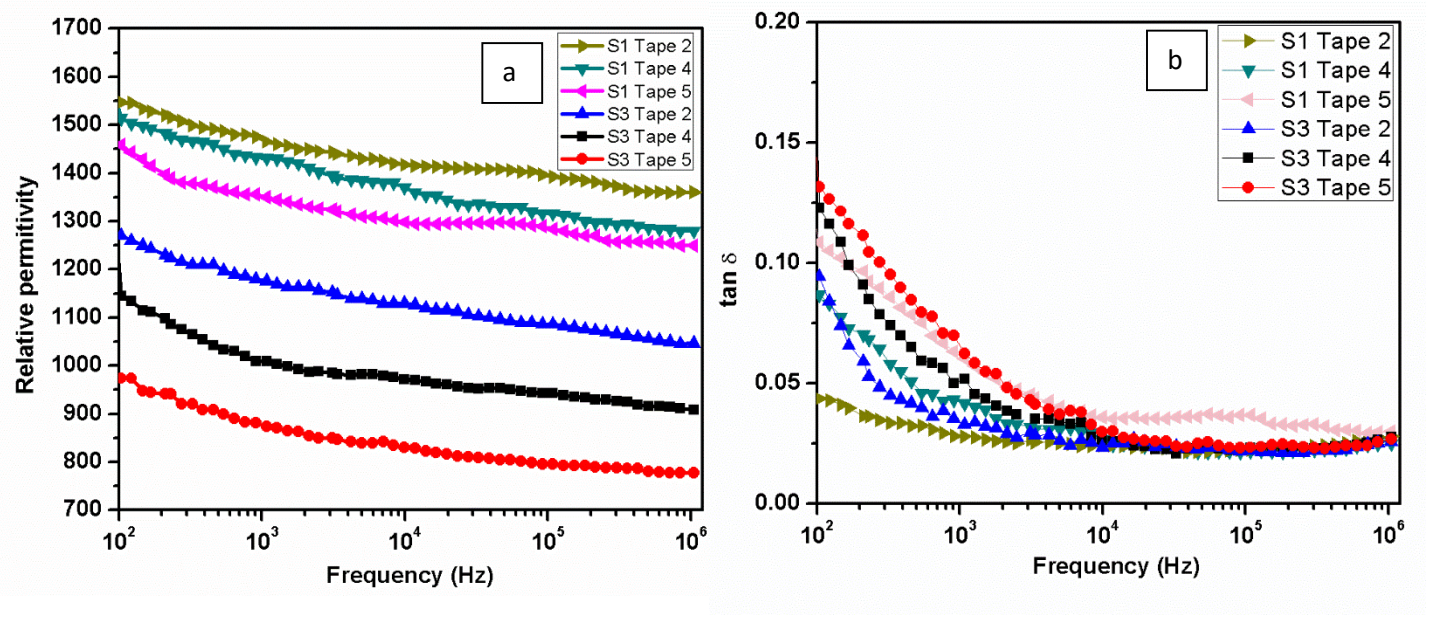

Figure 4.2.12 a) Relative permittivity b) Dissipation factor as a function of frequency for wafers sintered at 1450^{o}C/6h

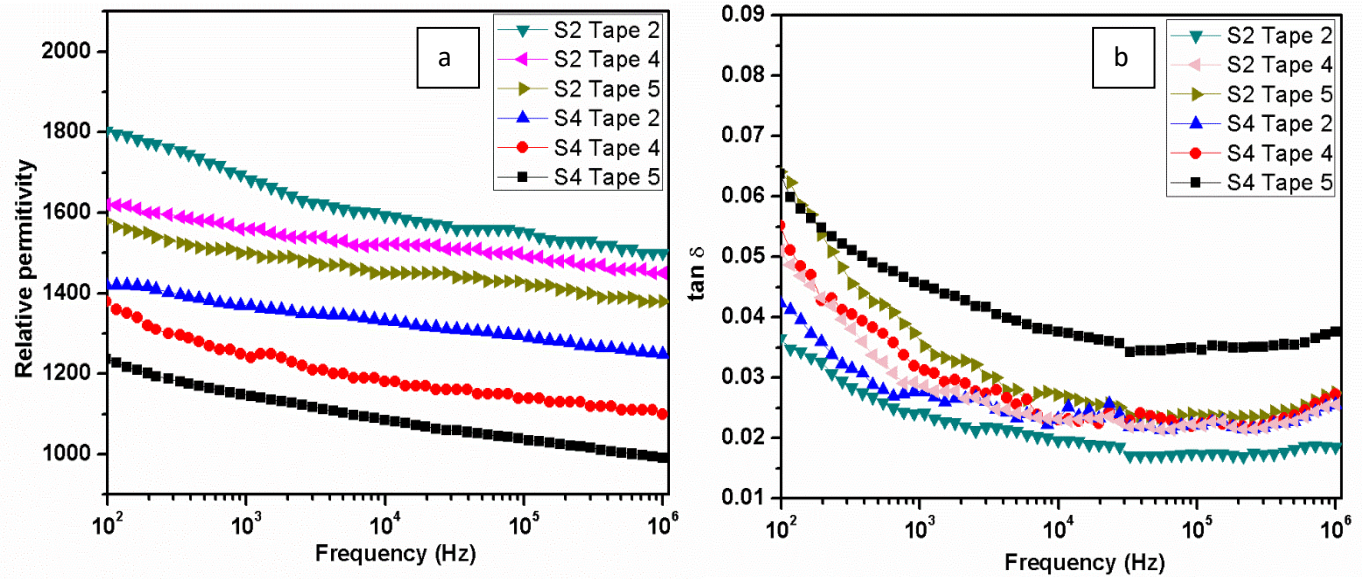

Figure 4.2.13 a) Relative permittivity b) Dissipation factor as a function of frequency for wafers sintered at 1500°C/4h

4.2.1.10 Ferroelectric and piezoelectric properties

Fig. 4.2.14 shows the polarization vs. electric field (P-E) loops of the Tape-2 and Tape-4 samples as the function of binder burn out temperature sintered at 1450°C/6h and 1500°C/4h. From the figure, it is clear that remanent polarization decreases with decrease in solid loading and density. Hysteresis loops are not well saturated for the samples sintered at 1450°C/6h, as the sintering temperature is increased to 1500°C/4h, well-saturated hysteresis loops are observed. That may be attributed to the better densification of the substrates at high temperature. Decrease in remnant and saturation polarization for 850°C binder burn out sample may be attributed to the lower density and higher concentration of phosphorous modified grain boundary. The piezoelectric properties of the different samples are shown in Table - 4.2.7. d_{33} of Tape-2 substrate is 172 pC/N, which is comparable to that of some Pb-free systems KNN, BNT-BT [33] and lower than that of bulk ceramics (discussed in section 1). In addition, d_{33} value further decreases with increase in binder burn out temperature to 850°C.

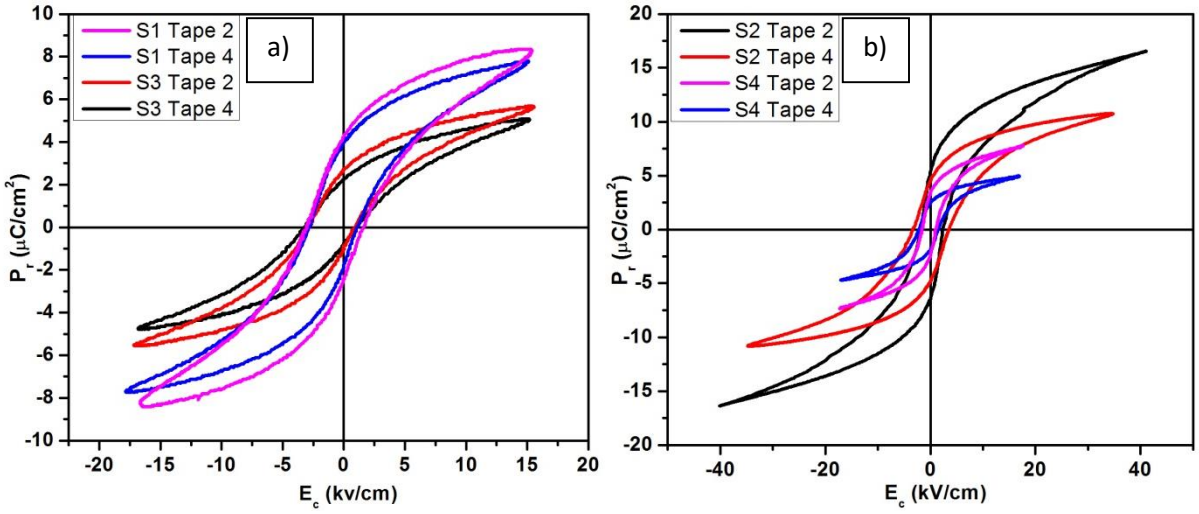

Figure 4.2.14 Shows the polarization vs electric field (P-E) loops of substrates sintered at different temperatures

Table 4.2.7 Variation of piezoelectric properties with solid loading

	d_{33}(pC/N)			
	S1	**S3**	**S2**	**S4**
Tape 2	130	86	172	132
Tape 4	98	63	120	98
Tape 5	62	40	75	60

Section – III Effect of PVB as a dispersant and binder on fabrication of tape and its electrical characterization

4.3 Introduction

In the previous section the non-aqueous tape casting of BZT-0.5BCT was studied by investigating the effect of dispersant (phosphate ester) and binder (PVB) content on the slurry rheology, the properties of tape cast BZT-0.5BCT layers, its densification, dielectric and piezoelectric properties. Phosphate ester (PE) is an effective dispersant for BZT-0.5BCT. However, the phosphate ester does not pyrolyse until the temperature 800^{o}C and may be some phosphorous remains that hampered the dielectric and piezoelectric properties of the substrates. Although PVB is a widely used binder, there have been some reports where this polymer is also used as a dispersant [32, 33].

In this section, an attempt was made to investigate PVB as a dispersant for BZT-0.5BCT powder in an MEK-EtOH azeotropic solvent system. The effect of PVB on dispersant properties as well as their effects on the properties of cast tapes, densification, and final electrical properties has been investigated. The rheological and electrical properties also have compared with substrate fabricated with phosphate ester as a dispersant.

4.3.1Effect of dispersant (PVB) on rheological behavior of BZT-0.5BCT slurry

The variation of viscosity of BZT-0.5BCT suspension with the concentration of dispersant (PVB) is shown in Fig. 4.3.1a. It is evident from the figure that the optimum dispersion was obtained at 0.5 wt% PVB concentration, which corresponds to a minimum in viscosity. Sediment height with dispersant concentration also followed the same trend (Fig. 4.3.1b). The sediment heights with days indicate that the slurries containing PVB around the optimum concentration (i.e., 0.5 wt%) remain more or less stable for 4 days and then start settling at a fast rate. PVB acts as a dispersant by steric stabilization mechanism [43, 44]. PVB dissolves in a solvent (MEK-EtOH) and anchored into the particle surface and extend the adsorbed long-chain into the solution to prevent the particles from approaching each other [45]. The decrease in viscosity is correlated with the coating of dispersant on the particles surface. The rise in viscosity with an increase in PVB concentration (above 0.5wt.% equivalent to 0.81 vol%) may be due to polymer bridging between the PVB molecules of nonionic nature [43]. Tseng et al. reported that 1wt% of PVB is sufficient to get stable suspensions of $BaTiO_3$ in MEK-EtOH solvent. Bhattacharjee et al. found that 0.6 vol%. of PVB required to stabilize $BaTiO_3$ suspension [43, 44]. In our case, we achieved stable suspensions at 0.5 wt% equivalent to 0.81 vol% of PVB.

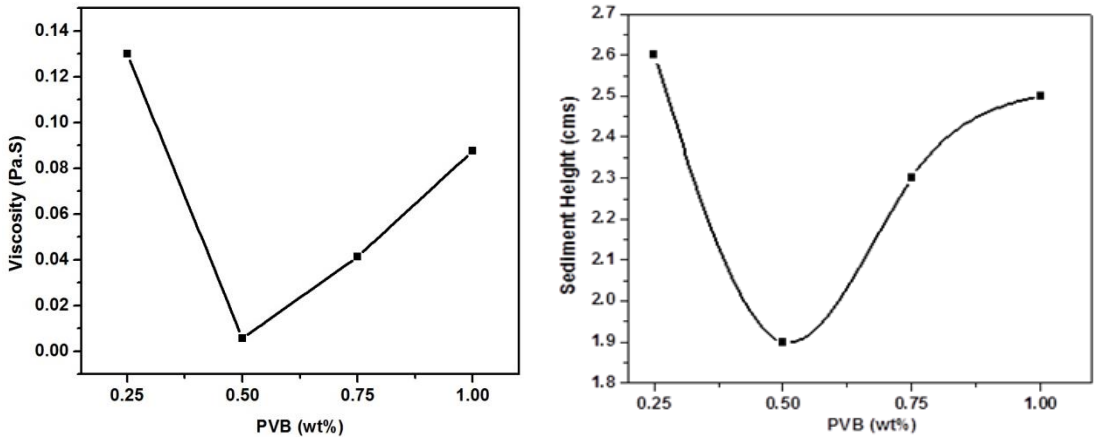

Figure 4.3.15 a) Effect of dispersant concentration on viscosity of slurry b) Effect of dispersant concentration on sediment height behavior

4.3.2 Study of rheological behavior of BZT-0.5BCT tape casting slurry

For preparation of tape casting slurry certain amount of binder (PVB) has to be added in addition to 0.5 wt% PVB, which is required for dispersion. In the previous section, it has been observed at least 3 wt% PVB required to get the good quality tape. The rheological study plays a vital role to understand the slurry processing. The viscosity of BZT-0.5BCT slurry (solid loading 59 wt. %) as a function of shear rate for different amounts (e.g. 2, 3, 4 wt.%) of the PVB is shown in fig 4.3.2. It is observed that the viscosity of slurry decreases with increase in shear rate. This behavior indicates shear thinning characteristics of the slurry. Viscosity also increases with the increase in PVB content of the slurry. This could be correlated to the powder agglomeration in the slurry. Shear rate exponent (n) of the slurry has been calculated using the power law model (discussed in section 2). The shear rate exponent values have been found to be in the range of 0.794-0.702 (Table 4.3.1). This indicates that all the slurries prepared in this study showed non-Newtonian behavior. In contrast, the tape casting slurry prepared with phosphate ester as a dispersant with higher solid loading (65 wt%) has lower shear rate exponent value (n= 0.473 for tape 2). It proves that PE is better dispersant compared to PVB for the preparation of the BZT-0.5BCT suspension.

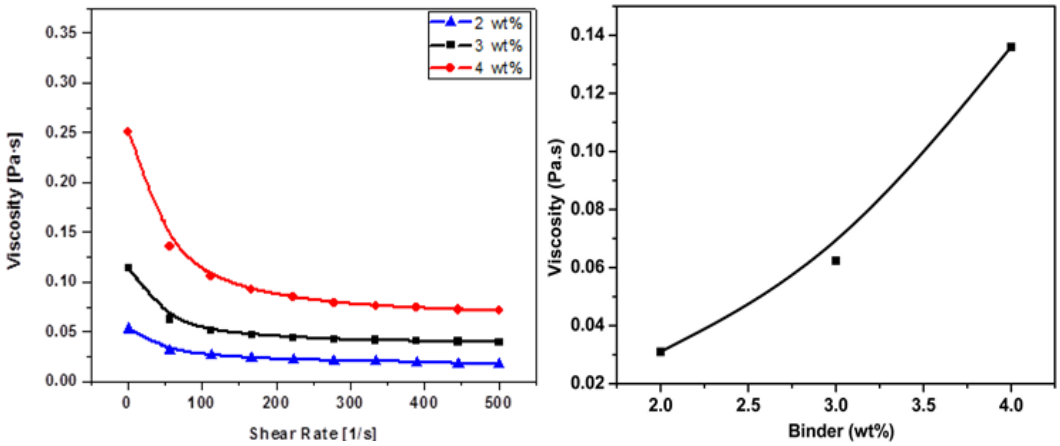

Figure 4.3.2 Effect of binder content on viscosity of slurry

Table 4.3.1 Effect of binder content on shear rate exponent

Binder wt%	Shear rate exponent (n)
2	0.7948
3	0.747
4	0.702

The shear-thinning (P) of a slurry is characterized by the ratio of the viscosities at 1 s^{-1} and 56.4 s^{-1}. When P = 1, the viscosity is constant, and the slurry presents Newtonian behavior. When P > 1, the bigger is P, the greater is the shear-thinning. From Table – 4.3.2, all the slurries show shear-thinning behavior. In contrast, the tape casting slurry prepared with phosphate ester as dispersant with higher solid loading (65 wt%) has higher shear rate exponent value (P = 5.26 for tape 2). However, the tape casting slurry prepared with PVB as dispersant and binder (0.5 and 3 wt%) could be casted easily when compared to other compositions having same solid loading.

Table 4.3.2 Shear thinning characterization of slurry

Binder wt%	P (ratio of viscosity at 1 s^{-1} and 56.4 s^{-1})
2	1.7065
3	1.9320
4	2.58

4.3.3 Physical appearance and microstructure of green tape

Fig 4.3.3 shows the physical appearance and micrographs of green tapes after drying. No visual defects were observed; the tape peeled off from the mylar sheet easily and had sufficient strength for handling.

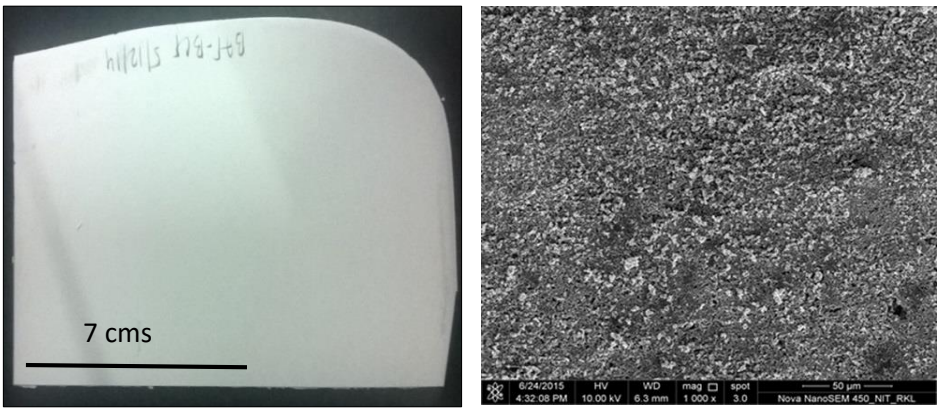

Figure 4.3.3 Physical appearance and micrograph of green tape

4.3.4 Thermal analysis of green tape

The thermo gravimetric (TG) analysis of the green tape is shown in Fig – 4.3.4. There is a marginal weight loss from room temperature to 200^{o}C. It can be attributed to the evaporation of the absorbed water and residual solvent. A sharp weight loss appears in the temperature interval between 200^{o}C to 300^{o}C. Another weight loss occurs in the temperature range of 300-500^{o}C. A small weight loss is observed around 600-700^{o}C. No major weight loss is observed beyond 700^{o}C. The PEG burns out at low temperature (< 300^{o}C) (Fig.4.3.18) followed by the second plasticizer, where decomposition arises between 240 and 380^{o}C because BBP has higher molecular weight compared to PEG and lower molecular weight compared to PVB [46]. The binder starts to decompose when the elimination of first plasticizer is complete. The burnout continues in only one step until 300^{o}C, and then a second step arises in the 300-500^{o}C temperature range due to binder removal and second plasticizer final decomposition [46]. Weight loss after 600^{o}C may be due to the presence of more binder that requires a higher temperature for complete decomposition.

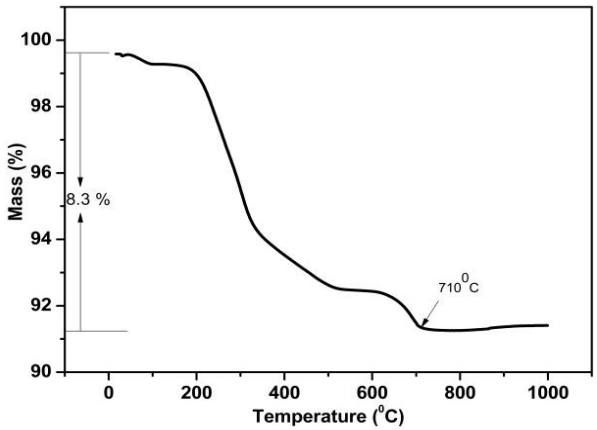

Figure 4.3.4 Thermal analysis of green tape

4.3.5 FESEM micrograph of sintered substrate

After binder burns out at 650ºC/2h, the substrates were fired at 1450ºC/6h and 1500ºC/4h. However, the relative density of substrates after sintering at 1500ºC was 93%. Fig 4.3.5 shows the FESEM micrographs of substrates sintered at two different temperatures. Substrate sintered at 1500ºC/4h shows dense microstructure compared with 1450ºC/6h sintered substrate. It is interesting to mention that the grain size of the sintered sample found to be 33 μm. In contrast, substrate fabricated with phosphate ester dispersant has a grain size of 15 μm for 850ºC binder burn out, and 24 μm for 650ºC binder burn out (section 2, page no.-77). It again corroborates our argument of retaining residual phosphorous and formation of phosphorus–BaO-rich phase that inhibits grain growth in substrates fabricated with phosphate ester as a dispersant.

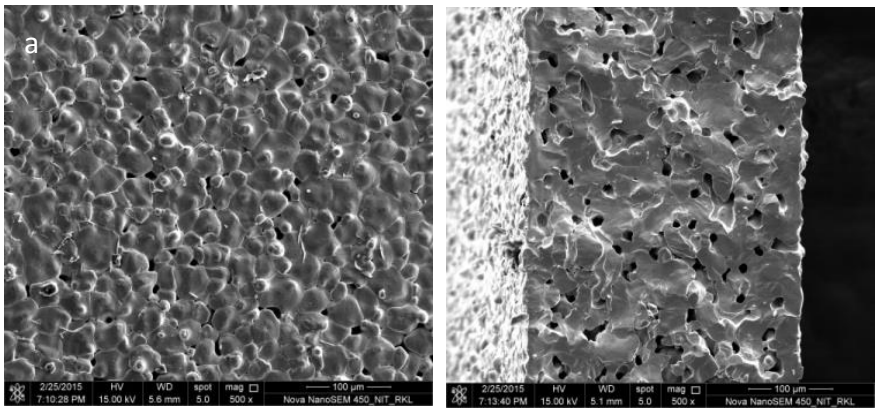

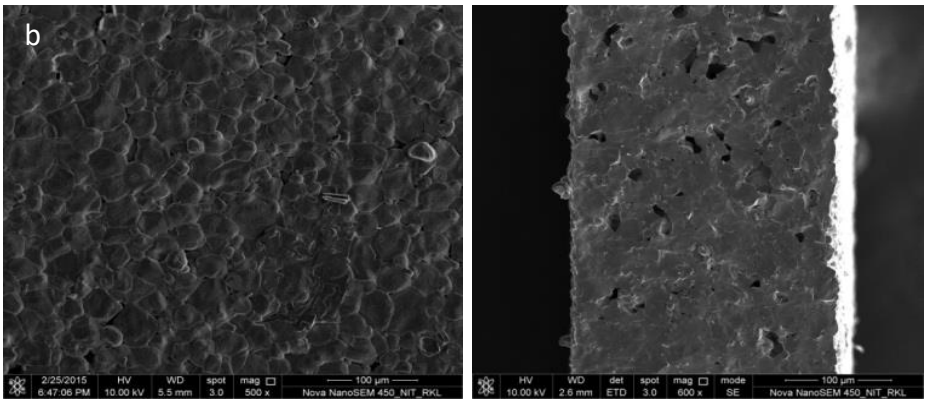

Figure 4.3.5 FESEM micrograph of substrate sintered at a) 1450^{0}C/6h b) 1500^{0}C/4h

4.3.6 Dielectric properties

Fig 4.3.6 & 4.3.7 shows the dielectric properties of the substrates fabricated with PE as dispersant and PVB as dispersant sintered at 1450^{0}C/6h and 1500^{0}C/4h as a function of frequency (100 Hz-1MHz). It can be observed that the room temperature relative permittivity values for BZT-0.5BCT substrates are 1530 and 1750 at 1kHz for 1450^{0}C/6h and 1500^{0}C/4h respectively. The loss factor of all the substrates is less than 2.5% at 1 kHz. The increase in relative permittivity with temperature can be attributed to increase in density of the substrates. It is interesting to mention that the substrates prepared with PVB as dispersant has better dielectric properties compared to phosphate ester as a dispersant. It is to be mention that Tape-4 has comparable solid loading (60 wt%) with Tape-PVB as dispersant (59 wt%). It is interesting to note that Tape-PVB has better dielectric properties compared to Tape-2 which has higher solid loading (65 wt%). Inferior dielectric property of substrates fabricated with phosphate ester as dispersant may be attributed to the presence of phosphorous-rich grain boundary phase.

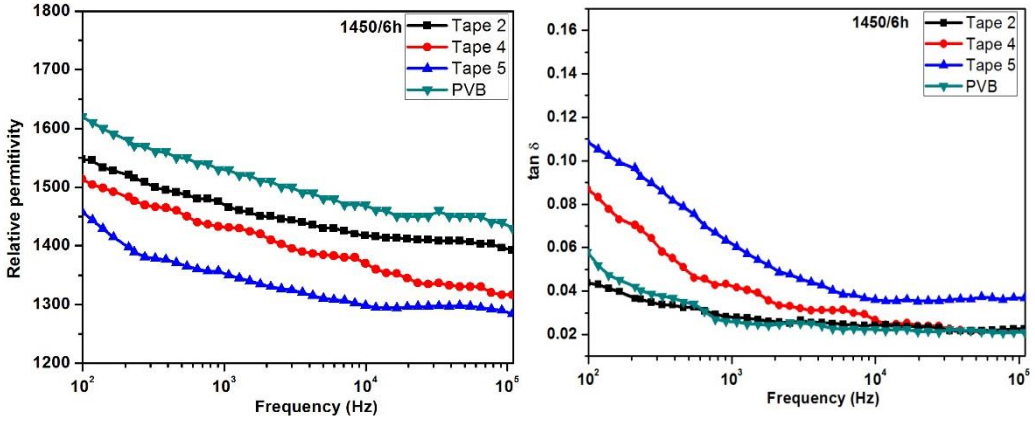

Figure 4.3.6 Relative permitivity and loss factor of substrates sintered at 1450^{O}C/6h

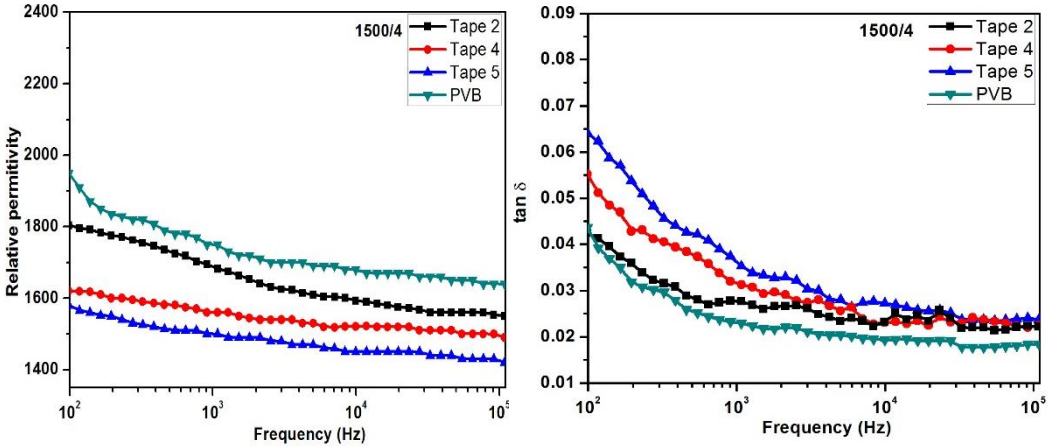

Figure 4.3.7 Relative permitivity and loss factor of substrates sintered at 1500^{O}C/4h

4.3.7 Ferroelectric and piezoelectric properties

Fig. 4.3.8 shows the polarization vs electric field (P-E) loops of the tape-PVB, tape-2 and tape-4 samples sintered at 1500°C/4h. Tape-PVB has well-saturated hysteresis loop, that may be attributed to the better densification of the substrates at high temperature. The wafer prepared using PVB as dispersant has better saturation and remanent polarization, compared to substrates prepared by using PE as a dispersant (Tape-4 with comparable solid loading). Piezoelectric constant (d_{33}) has also improved for tape-PVB and at par with tape-2 of higher solid loading. Table 4.3.3 shows the comparison of properties between substrates prepared by using PVB and PE as dispersants.

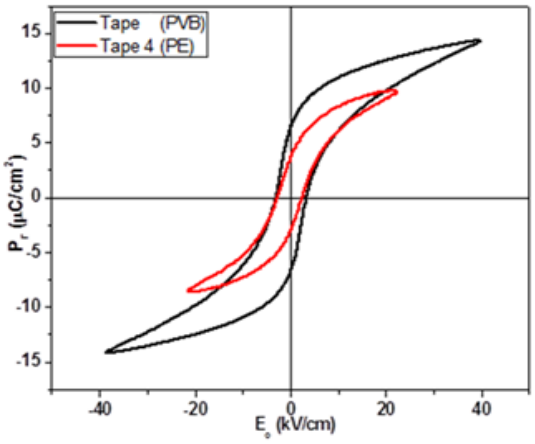

Figure 4.3.8 Polarization-electric field characterization of the BZT-0.5BCT

Table 4.3.3 Comparison of properties between substrates prepared by using PVB and PE as dispersants.

Serial no.	Solid loading wt (%)	$P_r(\mu C/cm^2)$	$E_c(kV/cm)$	d_{33}
Tape 4 (PE)	60	4.4	2.51	120
Tape (PVB as dispersant)	59	6.30	3.63	174

References

[1]. R. Yang, W. Fu. X. Deng, Z. Tan, Y. Zhang, L. Han, C. Lu, X. Guan, Adv. Mater. Res., 148, 1062-66, (2011).

[2]. P. Wang, Y. Li and Y. Lu, J. Eur. Ceram. Soc., 31, 11, 2005–2012, (2011).

[3]. W. F. Liu and X. B. Ren, Phys. Rev. Lett.10, 3257602, (2009)

[4]. F. Benabdallah, A. Simon, H. Khemakhem, C. Elissalde, and M. Maglione, J. Appl. Phys.109, 124116, (2011)

[5]. A. Srinivas, R. V. Krishnaiah, V. L. Niranjani, S. V. Kamat, T. Karthik, S. Asthana, Cer. Int. 41, 1980–1985, (2015).

[6]. W. Liu, X. Ren, Phys. Rev. Lett., 103, 257602, (2009)

[7]. W. Liu, Z. Xu, W. Ruiqing Chu, P. Fu, and G. Zang, J. Am. Ceram. Soc., 93, 10, 2942–2944 (2010)

[8]. X. G. Tang, Q.X. Liu, J. Wang, H. L. W. Chan, App. Phys., A, 96, 945-952, (2009).

[9]. N. Binhyeeniyi, P. Sukvisut, C. Thanachayanont, S. Muensit, Mat. Lett., 64, 305-308, (2010).

[10]. X. Lin, and F. G. Yuan, Smart Materials and Structure, 10, 907-913, (2001).

[11]. G. Park, D. J. Inman, Philosophical Transactions of the Royal Soc of Lon, 1-28, 365, (2007).

[12]. K. Uchino, Piezoelectric Actuators and Ultrasonic Motors, ed. H. Tuller, Kluwer Academic Publisher, Boston, p. 17, 33, (1997).

[13]. V. Giurgiutiu, J. of Min. Met & Mat. Soc 55, 10-11, (2003).

[14]. J. S Reed Principles of ceramics processing, John Wiley and Sons, 2nd edition. (1995).

[15]. R. E. Mistler, Tape casting theory and practice, The American Ceramic Society, (2000).

[16]. R. Moreno "The role of slip additives in tape-casting technology: Part I—Solvents and Dispersants" , J. Am. Ceram. Soc. Bull., 71, 1521–1531, (1992).

[17]. R. Moreno "The role of slip additives in tape-casting technology: Part II—Binders and Plasticizers" , J. Am. Ceram. Soc. Bull., 71, 1647–1657, (1992).

[18]. K.R. Mikeska and W.R. Cannon, Colloids and Surfaces, 29, 305, (1998).

[19]. W.R. Cannon, J.R. Morris and K.R. Mikeska, J. Am. Cer. Soc, p. 161, (1987).

[20]. V. Vinothini, P. Singh and M. Balasubramanian, International Symposium of Research Students on Mat. Sci. Eng. 2004, Chennai, India.

[21]. G. Jian, Q. Hu, S. Lu, D. Zhou and Q. Fu, Proc & App. Of Cer 6, 4, 215-221, (2012).

[22]. A Seal, D. Chattopadhyay, A. Das Sharma, A. Sen and H.S. Maiti, J. Eur. Ceram. Soc., 24, 2275-2283, (2004).

[23]. T. Chartier, E. Streicher, and P. Boch, Ceram. Bull., 66, 1653–1655, (1987).

[24]. J. A. Lewis, and A. L. Ogden, J. Am. Ceram. Soc., Westerville, 1995, pp. 361–365.

[25]. M. P. Brenner and P. J. Mucha Nature, 409, 568-569, (2001).

[26]. Z. Jingxian, J. Dongliang, L. Weisensel and P. Greil, J. Eur. Ceram. Soc.,24, 2259–2265, (2004).

[27]. E. Roncari, C. Galassi, F. Craciun, C. Capiani and A. Piancastelli, J. Eur. Ceram. Soc., 21, 409-417, (2001).

[28]. H. Raeder and C. Simon, J. Eur. Ceram. Soc.,13, 485-491, (1994).

[29]. Amit Mukherjee, B Maiti, A Das Sharma, R N Basu and H S Maiti, Cer Int., 27, 731-739 (2001).

[30]. Yingjie Qiao, Yingying Liu, Aidong Liu and Yan Wang, Cer Int., 38, 2319–2324, (2012).

[31]. E. Roncari, P. Pinasco, M. Nagliati and D. Sciti, J. Eur. Ceram. Soc., 24, 2303-2311, (2004).

[32]. W. J. Tseng and C. L. Lin. Mater, Let., 57, 223– 228, (2002).

[33]. S. Bhattacharjee, M. K. Paria and H. S. Maiti, J. Mater. Sci., 28, 6490-6495, (1993).

[34]. A. Sen, A. Seal, N. Das, R. Mazumder and H. S. Maiti, International Conference on Smart Materials Structures and Systems July 28-30, 2005, Bangalore, India

[35]. A. C. Caballero, J. F. Fernandez, M. Villegas, C. Moure, P. Duran, P. Florian and J. P. Coutures, J. Am. Ceram. Soc., 83, 6, 1499–505 (2000).

[36]. A. C. Caballero, J. F. Fernandez, C. Moure, P. Duran, Materials Letters, 35, 72–77, (1998).

[37]. A. C. Caballero, J. F. Femandez, P. Duran and C. Moure, J. Mat. Sci. 30, 3799 (1995).

[38]. W. Bai, B. Shen, F. Fu, J. Zhai, Thin Solid Films, 527, 110–113, (2013).

[39]. D. O. Neill, R. M. Bowman, J. M. Gregg, Appl. Phys. Lett. 77, 1520, (2000).

[40]. R.Mazumder, D.Chakravarty, D.Bhattacharya, A.Sen, Material Research Bulletin 44, 3, 555-559, (2009).

[41]. A. C. Caballero, J. F. Fernhdez, C. Moure and P. Duran, Materials Research Bulletin, 32, 2, 221-229, (1997).

[42]. T. R. Shrout, S. J. Zhang, J. Electroceram., 19, 111, (2007)

[43]. W. J. Tseng and C. L. Lin Mater, Let. 57, 223– 228, (2002).

[44]. S. Bhattacharjee, M. K. Paria and H. S. Maiti, J. Mater. Sci., 28, 6490-6495, (1993).

[45]. R. Moreno, J. Am. Ceram. Soc. Bull., 71, 1521–1531, (1992).

[46]. E. Roncari, P. Pinasco, M. Nagliati and D. Sciti, J. Eur. Ceram. Soc., 24, 2303-2311, (2004).

Chapter – 5

Conclusions & Scope of Future work

Conclusions

The following conclusions can be drawn from the present study

i) BZT-0.5BCT powder was prepared by solid-state reaction route. Effect of calcination temperature on phase formation and the particle size was studied. Perovskite phase was formed along with the impurity phases of $BaTi_4O_9$ and $BaTi_2O_5$ after calcination at 1000°C. Secondary phases significantly reduce after double calcination at 1000°C. The complete phase purity was obtained at 1200°C. The average agglomerate size increased from 0.4μm (double calcination at 1000°C) to 0.6 μm (single calcination at 1200°C) with increase in calcination temperature. The sintered ceramics prepared at 1500°C from double calcined powder (at 1000°C) and 1200°C calcined powder has comparable dielectric and piezoelectric property. The results show that the powder calcined at 1000°C (double calcined) and sintered at 1500°C exhibit good electrical properties: d_{33} = 470pC/N, ε_r= 3098 , and tan δ > = 0.0208, respectively.

ii) Dispersion of BZT-0.5BCT powder strongly depends on particle size. Double calcined (1000°C) powder with a particle size in the range of 0.27-0.5 micron is useful for preparation of tape casting slurry.

iii) From minima in slurry viscosity and sedimentation height, it was confirmed that 1wt.% phosphate ester is sufficient for effective dispersion of BZT-0.5BCT to get a stable slurry.

iv) The role of the binder (PVB) on rheological behavior of tape casting slurry, properties of the BZT-0.5BCT tape was studied. Variation of PVB content shows that at least 3wt% PVB required to get workable green tape. Up to 3.5 wt% PVB (binder) addition, solid loading can be maintained at 65%. With further addition of PVB, to get workable slurry solid loading has to be reduced.

v) Firing of green tapes was performed under load to avoid curling/warping of thin tape due to differential shrinkage during sintering. After optimization of the top load flat substrate can be found with a load of ~ 0.81 gm/cm^2.

vi) Density, relative permittivity and piezoelectric constant decreased with a decrease in solid loading. The highest density (94% of true density), relative permittivity (1700 at 1kHz) and piezoelectric constant (172 pC/N) has been obtained for tape with 3

wt% PVB content and 65% solid loading after firing at 1500^{o}C/4h.These properties are inferior to that of bulk BZT-0.5BCT. The presence of residual phosphorous and modification of the grain boundary may be the reason for degradation of the electrical properties.

vii) Tape casting was performed using PVB as a dispersant in place of the phosphate ester to check any detrimental effect of residual phosphorous in sintered specimen.

viii) From minima in slurry viscosity and sedimentation height, it was confirmed that 0.5 wt.% PVB is sufficient for effective dispersion of BZT-0.5BCT to get a stable slurry. However, increase in the shear rate exponent and decrease in shear thinning constant compared to the phosphate ester containing slurry indicates better dispersing ability of phosphate ester than PVB. Also, without using phosphate ester good quality tape can be prepared by tape casting.

ix) Improved dielectric (ε_r =1750 at 1 kHz), ferroelectric (P_r= 6.3 $\mu C/cm^2$) and piezoelectric properties were observed for wafers made without phosphate ester. The absence of residual phosphorous in grain boundary may be the reason for improvement of the electrical properties.

Scope of future work

- From this thesis, it is observed that stability of tape casting slurry strongly depends on the initial BZT-0.5BCT powder. In present study, solid loading cannot be increased beyond 65 wt%. It is also observed in our study that density of substrates is falling substantially with a reduction in solid loading and also degrading electrical properties. So, further work can be taken for the synthesis of BZT-0.5BCT powder below 0.2 microns in a large scale.
- Present thesis focuses on fabrication and characterization of the BZT-0.5BCT substrate. With this knowledge base, multilayer actuator based on the BZT-0.5BCT composition can be fabricated.
- Best wafer prepared from our study can be used for further studies on Lamb wave excitation and sensing.
- Co-Firing of the electrode (Platinum and gold) with the green substrate has to be studied for fabrication of multilayer actuators.

RESUME

S.Abhinay

Mobile: +91-8895764502, 7504405405 **Email:** abhinaysrrm94@gmail.com;
DOB: 22nd Feb, 1991

EDUCATIONAL CREDENTIAL

B.Tech (Ceramic Technology) 2012

Andhra University, Visakhapatnam; CGPA 7.95

Intermediate (M.P.C) 2008

Gowtham junior college, Guntur, Andhra Pradesh, 90.2%

Matriculation 2006

Gopi Krishna High school, Proddatur, Andhra Pradesh, 85.6%

List of publications related to the thesis

1. A.Sreeram, A. Seal, R. Mazumder, A.Sen "Fabrication of BZT-0.5BCT Piezoelectric Wafers by Tape Casting Technique and Their Characterization" (Under review)
2. A.Sreeram, A.Seal, R. Mazumder, A.Sen "Effect of Two Different Dispersants on Fabrication of BZT-0.5BCT Piezoelectric Wafers by Tape Casting Technique" (Under preparation)

List of presentations in Conferences

1. S. Abhinay, A. Seal, R. Mazumder, A. Sen "Fabrication of BZT-BCT Piezoelectric Wafers by Tape Casting Technique and Their Characterization" AMF-AMEC-2014 The Joint Conference of 9th Asian Meeting on Ferroelectrics & 9th Asian Meeting on Electroceramics, Oct. 26-30, 2014, Shanghai, China, p 66.
2. S. Abhinay, A. Seal, A. Sen, R. Mazumder "Effect of Two Different Dispersants on Fabrication of BZT-BCT Piezoelectric Wafers by Tape Casting Technique" 1st International Conference on "Alumina and other Functional Ceramics (AOFC-2015)" 11-13 March, 2015, Central Glass and Ceramic Research Institute, Kolkata.